

# **SILVERWARE SINGULATION SYSTEM**

By

**Rajashekar Reddy Chitaveli**

Bachelor of Engineering

Visvesvaraya Technological University

Bangalore, Karnataka, India

2007

Submitted to the Faculty of the

Graduate College of the

Oklahoma State University

in partial fulfillment of

the requirements for

the Degree of

**MASTER OF SCIENCE**

December, 2011

# SILVERWARE SINGULATION SYSTEM

Thesis Approved:

Dr. Lawrence Hoberock

---

Thesis Adviser

Dr. Martin Hagan

---

Dr. Ronald D. Delahoussaye

Dr. Sheryl A. Tucker

---

Dean of the Graduate College

# TABLE OF CONTENTS

Chapter	Page
<b>1. INTRODUCTION .....</b>	<b>01</b>
1.1. Review of Previous Work at Oklahoma State University .....	02
1.2. Patent Review .....	03
1.3. Previous Singulation Work – Akella (2008) .....	05
1.4. Objective .....	10
<b>2. DESIGN OF SILVERWARE SINGULATING SYSTEM .....</b>	<b>11</b>
2.1. Problems Identified With the Existing Setup .....	11
2.2. Initial Experiments .....	12
2.3. Concept .....	13
2.4. Design of Conveyor Feed Bin .....	15
2.4.1. Speed and Torque Calculations of Conveyor .....	15
2.4.2. Selection of Roller Shafts, Stepper Motor and Belts .....	18
2.5. Selection of Silverware Sensors .....	23
2.5.1. Investigation of Non-Contact Sensors .....	23
2.5.2. Investigation of Inductive Proximity Sensors .....	26
2.5.3. Design of Sensor-Bed .....	32
2.6. Selection of Material for Stage02 .....	39
<b>3. DESIGN OF CONTROL SYSTEM .....</b>	<b>45</b>
3.1. Speed Control of a DC Stepper Motor .....	46
3.2. Description of Hardware and Software .....	50
3.3. Coordination of Sensors, Stepper Motor, Electromagnets and Solenoid .....	53

<b>4. EXPERIMENTAL RESULTS .....</b>	<b>56</b>
4.1. Singulating Efficiency and Throughput at Various Belt Speed.....	58
4.2. Singulating Efficiency Results without Sensor Bed-1, Sensor Bed-2 and Electromagnets at Various Belt Speeds .....	63
4.3. Singulation Test with Metering Bin .....	68
4.4. Discussion of Results .....	68
<b>5. Conclusions and Recommendations .....</b>	<b>72</b>
5.1. Contributions .....	73
5.2. Drawbacks .....	74
5.3. Recommendations .....	75
<b>REFERENCES .....</b>	<b>76</b>
<b>APPENDICES .....</b>	<b>77</b>
Appendix – A Abstracts of Patents Reviewed .....	78
Appendix – B Websites Referenced .....	81
Appendix – C Datasheet for Conveyor Feed Bin Stepper Motor .....	83
Appendix – D Datasheet for Stepper Motor Driver .....	86
Appendix – E Datasheet for Inductive Proximity Sensor .....	89
Appendix – F Pin Diagram – PIC 18f4520 .....	98
Appendix – G PIC C Code for Silverware Singulation .....	101
Appendix – H Datasheet for Motor Belt Drive .....	109
Appendix – I Datasheet for the Solenoid .....	111

## LIST OF TABLES

<b>Table</b>	<b>Page</b>
2.1 Weight of each type of silverware .....	16
2.2 Correction Factors for different materials .....	29
3.1 Truth for Sensor Configuration, Akella (2008) .....	53
4.1 Singulating Results for Magnet Rate of 52 magnets/min .....	58
4.2 Singulating Results for Magnet Rate of 59 magnets/min .....	59
4.3 Singulating Results for Magnet Rate of 67 magnets/min .....	59
4.4 Singulating Results for Magnet Rate of 76 magnets/min .....	60
4.5 Singulating Throughput for Magnet Rate of 52 magnets/min .....	61
4.6 Singulating Throughput for Magnet Rate of 59 magnets/min .....	61
4.7 Singulating Throughput for Magnet Rate of 67 magnets/min .....	62
4.8 Singulating Throughput for Magnet Rate of 76 magnets/min .....	62
4.9 Singulating Results without Electromagnets for Magnet Rate of 76 magnets/min .....	63
4.10 Singulating Results without Electromagnets for Magnet Rate of 67 magnets/min .....	64
4.11 Singulating Results without Electromagnets for Magnet Rate of 59 magnets/min .....	64
4.12 Throughput Results without Electromagnets for Magnet Rate of 76 magnets/min .....	66
4.13 Throughput Results without Electromagnets for Magnet Rate of 67 magnets/min .....	66
4.14 Throughput Results without Electromagnets for Magnet Rate of 59 magnets/min .....	67
5.1 Efficiency and Throughput of Akella's machine, (2008) .....	72
5.2 Efficiency and Throughput of Present Setup .....	73

## LIST OF FIGURES

Figure	Page
1.1: Flatware Separating Apparatus U.S. Patent 4,954,250 (1999) .....	04
1.2: Flatware Sorting machine U.S. Patent 5,996,809 (1999) .....	05
1.3 Sketch of V. Akella's Silverware Singulating Machine (2008 .....	07
1.4 Sketch of Comb Pattern of Sensor Circuit, Akella (2005) .....	08
2.1 NEMA Size 34 Round Stepper Motor .....	19
2.2 MBC 12101 Microstep Driver .....	20
2.3 Stepper Motor and Driver Shaft Assembly .....	21
2.4 Hammer-In Alligator Lacing .....	22
2.5 IR Sensor Operation .....	24
2.6 Components of Inductive Proximity Sensor .....	27
2.7 Sensing Area Diagram of an Inductive Proximity Sensor .....	28
2.8 Shielded (Top) and Unshielded (Bottom) Proximity Sensor with Their Magnetic Fields .....	30
2.9 Mutual Interference of Inductive Proximity Sensors .....	31
2.10 NPN and PNP Output .....	33
2.11 Opposed positioning of sensors .....	35
2.12 Layout of Sensor Bed .....	37
2.13 Inductive Proximity Sensor PBT-AP-2H .....	38
2.14 Top View of Side by Side Positioning of Sensors in Sensor Bed .....	38

2.15 Side View of Masonite Downward Incline Plate, with Sensors and Electromagnets .....	39
2.16 Damaged 150 x 150 (top) and 200 x 200 (bottom) Mesh Wire Cloth .....	41
2.17 Combination of Plastic sheet with Teflon Cloth .....	42
2.18 Sketch of Present Setup .....	44
3.1 Waveform Output of a Timer .....	45
3.2 Circuit Diagram for the Silverware Singulation Setup .....	51

Name: Rajashekar Reddy Chitaveli

Date of Degree: December, 2011

Institution: Oklahoma State University

Location: Stillwater, Oklahoma

Title of Study: SILVERWARE SINGULATION SYSTEM

Pages in Study: 113

Major Field: Mechanical and Aerospace Engineering

Scope and Method of Study:

Singulation of silverware, means to 'single out' individual pieces of silverware pieces from a mixed batch of silverware, consisting of spoons, soup spoons, knives and forks. The objective of this research is to modify, design, construct and test an efficient automated mechanism to singulate silverware pieces, starting with Akella's (2008) machine. The process of singulation was sub-divided into two stages:

1. Stage-01: Divides the batch of 400 silverware pieces into smaller batches of approximately 20 pieces each, which I accomplished by employing a slow moving conveyor belt, inductive proximity sensors and electromagnets. A mixed batch of silverware pieces is spread on the conveyor belt, which feeds them to a downward inclined plate. The electromagnets beneath the inclined plate holds the silverware pieces to the inclined plate, or releases them, depending on the output signals of inductive proximity sensors, which are also placed beneath the inclined plate.
2. Stage-02: Singulates silverware pieces from these smaller batches. A metering bin collects the silverware pieces from the downward inclined plate. A pulsed solenoid vibrates the metering bin by striking the bin bottom. This causes the silverware pieces to move out through the open end of the bin onto a plastic lined Teflon cloth. This cloth is placed above a moving leather belt carrying a series of hemispherical permanent magnets, such that the silverware pieces attracted by one of the magnets slides along the cloth to exit the machine.

Findings and Conclusions:

An efficient singulating mechanism has been designed and developed.

Conveyor feed bin improved the feeding mechanism to deliver silverware pieces to the inclined plate. Inductive proximity sensors were researched, and the sensor beds were designed and developed to provide a reliable feedback to various actuators in the rig.

Effectively used plastic lined teflon cloth as a covering material for the moving magnet on the leather belt, which offered improved wear resistance. Singulating efficiency of 97% and throughput of 44 pieces/min were achieved.

ADVISER'S APPROVAL: Dr. Lawrence Hoberock

---



# CHAPTER 1

## INTRODUCTION

An automatic dishwasher is a common household device used to batch-clean utensils and dishes. Automatic commercial dishwashers, however, used in restaurants, hotels, hospitals, and other institutions, are designed differently to clean dishes in a continuous, non-batch process. Commercial dishwashers perform the primary function of cleaning, but for post-dishwashing operations such as inspection and sorting, manual labor continues to be used. Manual processing is undesirable because of the harsh environmental conditions, repetitive nature of the work leading to poor efficiency, increased cost of operation, and absenteeism. Automation of post-dishwashing operations holds promise for reduced labor, reduced operating costs, and increased productivity (Peddi, 2005).

The present topic has been motivated by a typical commercial dishwashing operation in a private 700 bed hospital in the mid-western U.S (Hashimoto 1995; Nagaraj 2003). This hospital operates 3 two hour dishwashing shifts daily, each processing up to 700 trays of dishes per shift. Each tray typically consists of four silverware pieces, a spoon, a soup spoon, a fork, and a knife, amounting to 2800 silverware pieces per shift, and 8400 pieces per day.

The post-dishwashing operation can be roughly broken down into three functions: singulation, inspection, and sorting. Complex geometries of silverware present challenging areas of research in automation of these three functions.

### **1.1 Review of Previous Work at Oklahoma State University**

Separation, referred to as singulation of silverware, means to 'single out' individual pieces from a mixed batch. Inspection distinguishes clean from dirty silverware. Sorting involves placing the spoons, soup spoons, knives and forks into separate bins with appropriate orientation. A final operation consists of wrapping the set of silverware in a napkin.

Hashimoto (1995) built a silverware singulating machine with a singulation percentage of 41% and alignment percentage of 14.9%. Singulation percentage refers to the percent of individual pieces of silverware separated from a mixed batch. Alignment percentage refers to the percent of silverware pieces that were processed in the correct orientation from a mixed batch. Akella (2008) improved upon Hashimoto's results, yielding a singulation percentage of 92.9%, an alignment percentage of 100%, and an average throughput of 28.41 pieces/min.

Yerri (2003) developed a vision system to identify the different types of silverware that yielded 100% accuracy. Lolla (2005) built a vision system to inspect the cleanness of the silverware which yielded 87% and 91% inspection accuracy for clean and dirty silverware respectively, and processed at a rate of 55 pieces/min.

Nagraj (2003) built a device for sorting silverware into 4 different groups with a sorting efficiency of 91.6% and processed at a rate of 21 pieces/min. Peddi (2005) improved on Nagraj's results with a sorting efficiency of 91.6% and processing rate of 45 pieces/min.

Jeyapalan (2005) devised a method to wrap a set of silverware in a napkin that produced an 68% correct wrapping. Lertrit (2010) developed a mechanism to produce sets of silverware at a rate of 5.40 sets of silverware/min, and the machine was 100% successful in forming complete silverware sets.

## **1.2 Patent Review**

Key words- "silverware singulation", "singulate silverware", "separate silverware", "sort flatware" and "flatware separate" were used to search through United States patents.

There were not many results for singulation, but numerous results were found for sorting U.S. Patent 4,954,250 "Flatware Separating Apparatus" Sep. 04, 1990, shows an apparatus in Fig 1.1 that houses a track onto which the silverware is directed to go past a stream of fluid which separates the knives from spoon and forks. The combination of spoons and forks is then routed to a pair of rollers whose width is sufficient enough to let the forks to let through and hold back the spoons. This apparatus lacks an inspection system and is prone to silverware jamming.

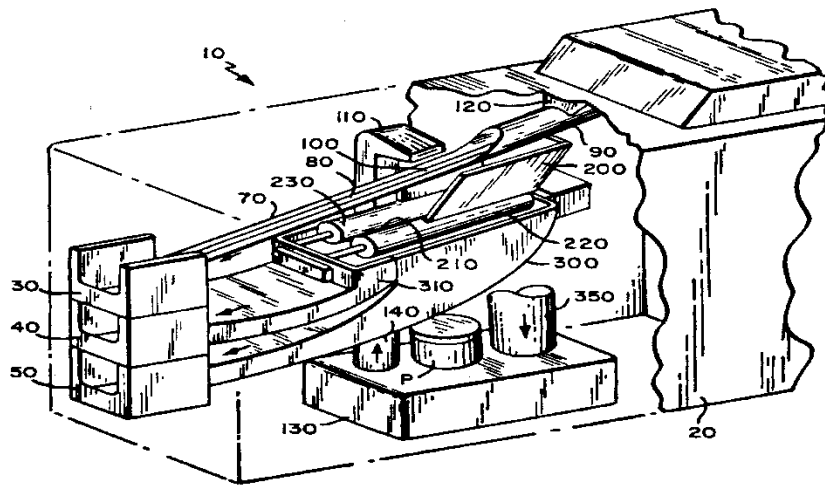


**Fig 1.1: Flatware Separating Apparatus U.S. Patent 4,954,250 (1999)**

U.S. Patent 5,996,809 “Flatware Sorting machine”, Dec. 07, 1999, has the objective of sorting flatware according to type and orientation, illustrated in Fig 1.2. The feed bin (12) holds disoriented silverware. The flatware pick up system employs suspended magnets to pick up individual pieces of silverware and transports them into the sorting system, where each piece of silverware is vertically dropped into the appropriate feed hopper, purportedly ensuring the correct orientation. This apparatus is not suitable for our application, since it does not inspect the silverware, jams may occur due to narrow slots, and more than one piece of silverware may be picked by the suspended magnets.

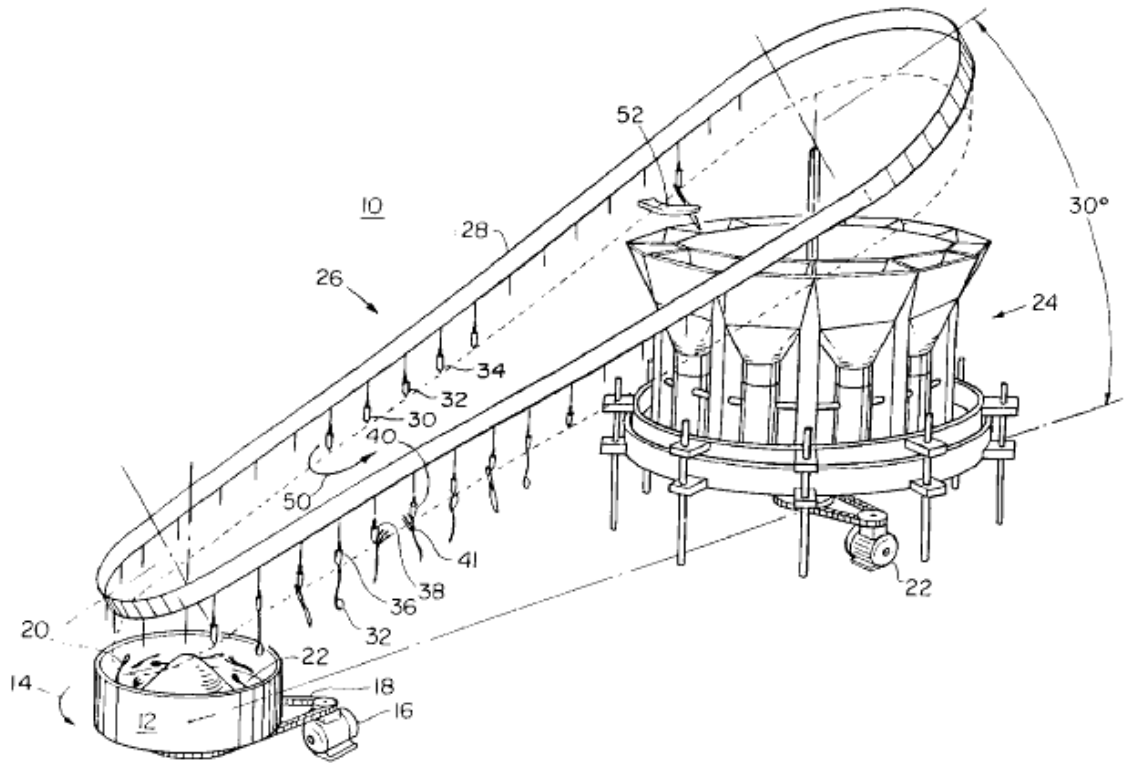


**Fig 1.2: Flatware Sorting machine U.S. Patent 5,996,809 (1999)**

### 1.3 Previous Singulation Work – Akella(2008)

Akella (2008) proposed a new method for separation of mixed silverware in a batch. His prototype could handle 400 pieces per batch. A schematic of his device is shown in Fig. 1.3, with (1) being the feed bin. The feed bin containing the mixed batch was made of masonite sheet and had dimensions of 24"x14"x8". Mixed silverware pieces were loaded into the bin which was vibrated in the direction parallel to the bin bottom using a crank pin mechanism driven by a 24V motor. The vibratory motion conveyed pieces slowly out the open end of the bin.

The vibrating was tested under 2 inclinations of the bin bottom plane:

1.  $0.93^\circ$  up with respect to horizontal.
2.  $1.85^\circ$  down with respect to horizontal

The vibrating frequency of the bin was 2.58 Hz, with a stroke of 0.5".

As indicated in Fig 1.3, silverware is transferred from feed bin (1) to a downward sloping Masonite plate (3) inclined  $20.7^\circ$  below horizontal with the dimensions of 40.5"x11.125". Two electromagnets were placed under the masonite inclined plate to act as non-intrusive gates for silverware pieces sliding over them. They could be turned on and off to control the flow of silverware sliding down the plate. Following the inclined plate, silverware passed into a metering bin (4). This bin, made of poster board with dimensions 14"x9"x7", was used to further regulate silverware flow. The bottom of this bin was inclined  $15^\circ$  below horizontal and was vibrated normal to the bin bottom by a solenoid plunger, such that when the silverware dropped into the metering bin, the pulsing solenoid vibrated the base of the bin to help move silverware pieces out.

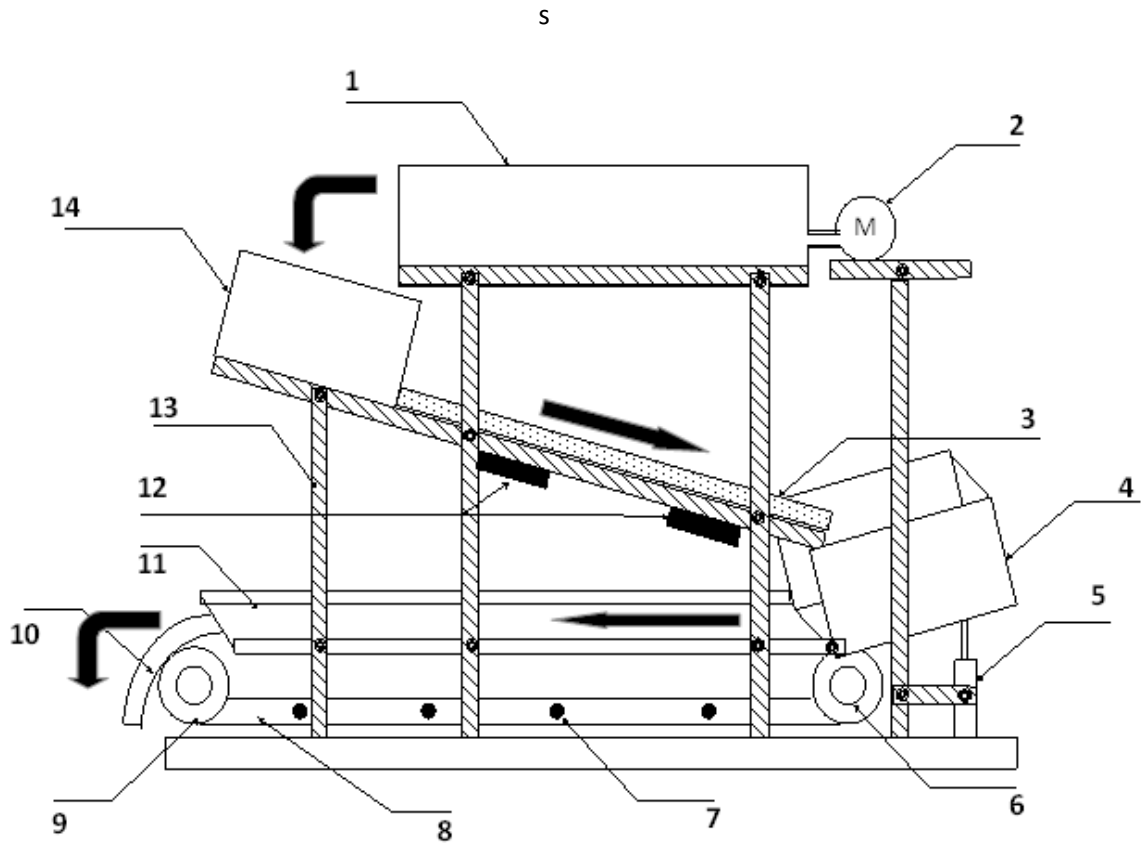


**Fig 1.3 Sketch of Akella's Silverware Singulating Machine (2008)**

**Bold arrows indicate silverware flow**

- |                                     |                            |
|-------------------------------------|----------------------------|
| 1. Feed Bin                         | 2. Motor for Vibrating Bin |
| 3. Masonite Downward Inclined Plane | 4. Metering Bin            |
| 5. Solenoid                         | 6. Driver Roller           |
| 7. Hemispherical Magnets            | 8. Belt                    |
| 9. Driven Roller                    | 10. Scraper                |
| 11. Duck Cloth                      | 12. Electromagnets         |
| 13. Aluminum Frames                 | 14. Receiving Bin          |

Akella (2008) developed sensors consisting of a striped comb pattern of flat copper conducting strips on a substrate, shown in Fig 1.4. This pattern of strips was connected in an open circuit, but when a conducting material such a silverware piece contacts at least two strips on opposite sides of the comb structure, the circuit is closed. A voltage signal from the closed circuit was used to indicate presence of silverware. Three such sensor circuits were used: two on the Masonite downward inclined plate (12) over each electromagnet and one in the bottom of the metering bin.

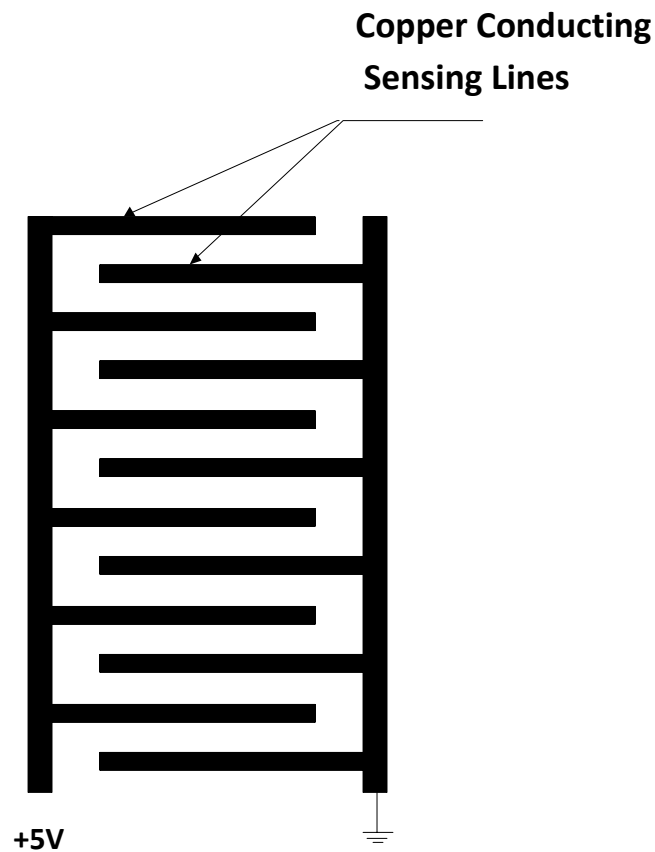


**Fig 1.4 Sketch of Comb Pattern of Sensor Circuit, Akella (2005)**

As shown in Fig 1.3, the downward inclined plate (3) was used to help break into smaller batches silverware pieces leaving the feed bin. Then, silverware entered the metering bin



(4), which helped further reduce batch size. Upon leaving the metering bin silverware fell onto a duck cloth strip (11), beneath which was a moving belt (8) containing serially placed hemispherical permanent magnets (7). These magnets were mounted on a leather belt, which was a continuous strip traversing two pulleys, one of which was driven by a variable speed electrical motor. The hemispherical magnets were glued to the top of the belt 10" apart. Duck cloth was placed above the belt such that silverware pieces attracted by a magnet were pulled in sliding action along the cloth. Akella (2008) investigated a wide variety of carrying materials before selecting the duck cloth. The belt motor voltage inputs could be varied among 18V, 21V, 24 V and 27V, and the respective line speeds of the belt magnets were 52, 59, 67 and 76 magnets/min respectively. With this device Akella (2008) achieved an average singulating speed of 28.41 pieces/min with an average singulating efficiency of 92.41%

**Disadvantages:**

- The delivery of silverware pieces from the feed bin (1) to the downward inclined plate (3) was discontinuous, caused by dense and uneven silverware mix in the batch, and by uneven vibratory feeding.
- The copper strips in the silverware sensors Fig. 1.4, were easily worn and damaged by sliding silverware pieces. Heavier damage occurred to the copper strips in the metering bin caused by both impact and sliding of silverware pieces. Moreover, friction between the copper strips and silverware pieces frequently prevented the

silverware pieces from sliding down the inclined plate during the absence of the magnetic field, when the electromagnets (12) were turned off.

- The duck cloth was not durable with repeated use. Forks, in particular, initiate damage when they slide with their tines facing down, and the duck cloth was then further damaged as other pieces slid over the already damaged portion.

#### **1.4 Objective**

Because the Akella machine (2008), Fig. 1.3, appeared to perform significantly better than any previous singulation process, we elected to use its basic concept. The objective of this thesis is to modify, design, construct and test an efficient mechanism to singulate silverware pieces, starting with Akella's (2008) machine, Fig. 1.3. Specific goals are

- Use the basic concept of Akella to modify the silverware singulation machine to improve the singulating speed and singulating efficiency.
- Improve the feeding mechanism to deliver silverware pieces more uniformly to the inclined plate (3).
- Improve silverware sensing on the inclined plate (3) and the metering bin (4) to prevent wear of sensor elements and eliminate friction that prevents silverware from easily sliding down the inclined plane.
- Investigate means other than duck cloth (11) to prevent wear.

Chapter 2 presents basic concepts and our final design to meet these goals.

## **Chapter 2**

### **Design of Silverware Singulating System**

#### **2.1 Problems Identified with Existing Setup**

Akella's (2008) machine achieved an average singulating speed of 28.41 pieces/min with an average singulating efficiency of 92.41%, but there were several shortcomings, which needed further research. Those were:

- Non uniform dispensing from the feed bin
- Erosion of sensor circuits on the masonite downward inclined plate and metering bin
- Friction from the sensor circuits decreased the flow of silverware on the downward inclined plate
- Wear of the duck cloth due to the friction caused by silverware, primarily by forks

These drawbacks suggested ideas to improve Akella's silverware singulation set up (2008). We felt the feed bin could be replaced by a mechanism that distributed silverware more uniformly to the inclined plate. The erosion of the copper sensing strips in the comb circuit was a major concern, leading us to investigate a more rugged design or eliminate altogether the contact between the silverware and the sensor circuit. By choosing the latter, we could also eliminate

the friction between the sensor circuits and silverware pieces. Finally, we felt investigation of materials to replace the duck cloth for longer durability would add improvement. The factors to be considered in the selection of the material to replace the duck cloth are friction between silverware pieces and the material, magnetic permeability, rigidity of the material, cross-sectional thickness, and durability to wear.

## **2.2 Initial Experiments**

To control the non-uniform dispensing from the feed bin, a belt conveyor to replace the vibrating feed bin was considered as a plausible solution. We performed initial experiments with the variable speed horizontal belt conveyor from Hytrol Conveyor Company, Model TA, that was available in our lab. Specifications are:

- Drive Pulley - 4 inch diameter with 1 inch diameter shaft at bearings
- Tail Pulley - 4 inch diameter with 1 inch diameter shaft at bearings
- Motor - 1/3 HP
- Belt Width - 30 inch

An area of 11" x 50", which was the overall width and length of Akella's machine (2008), was marked with chalk on the belt conveyor. Following Akella (2008), we selected the size of the silverware batch as 400 pieces and spread this batch as evenly as possible over the marked area. The belt conveyor's original speed was 3.75 inch/sec, for which the flow of silverware was observed. We determined from observation that this speed would be too high for dispensing the silverware at a reasonable rate (as determined by Akella, (2008)) to the inclined plate. To achieve a singulation speed of 35 pieces/min, the ideal conveyor speed was calculated to be

0.07 inch/sec, as shown in Section 2.4.1. Hence, an attempt was made to reduce the speed of the belt conveyor, using the adjustable belt and pulley alignment provided with the conveyor. The lowest achievable conveyor speed was 2.44 inch/sec, which was still too high for our needs, however, observations of silverware pieces discharged from the conveyor gave us confidence that a belt conveyor moving at a sufficiently slow speed might work to provide more even feed to the inclined plate.

### **2.3 Concept**

Akella (2008) proposed that the process of singulation should be sub divided into two stages:

- 1. Stage-01:** Divide the batch of 400 silverware pieces into smaller batches of approximately 20 pieces each
- 2. Stage-02:** Singulate silverware pieces from these smaller batches

**Stage-01:** Appropriate electromagnets and sensors are employed to divide the batch of 400 silverware pieces into smaller batches of approximately 20 pieces. By employing a slow moving conveyor belt, we found that we could spread out the silverware pieces on the conveyor, which would then feed silverware pieces to the masonite downward inclined plate in a more uniform and controlled manner than Akella (2008) could achieve using a vibratory feeder. The electromagnets beneath the inclined plate produce variable magnetic force by varying the current to the electromagnet. These can be switched on or off at a fast rate depending on the output of the silverware sensors. The same electromagnets [Coil Technologies, Part # E-0379-4] used by Akella (2008) were retained for the project herein, with the following specifications:

- Each lifts 962 lb. at 24v DC and 879 lb. at 12v DC.

- Each operates at 50% duty cycle at 24v DC and continuous duty cycle at voltages up to 10v DC.

The copper strip sensors used by Akella (2008) were replaced by inductive proximity sensors.

Section 2.5.2 describes the various sensor alternatives we investigated, leading to our choice of inductive proximity sensors and their selection and sizing. Section 2.5.3, describes positioning of these sensors. Following Akella (2008) we selected two sensor beds below the inclined plate and one below the metering bin. Again following Akella (2008), the electromagnets are turned on and off depending on the presence or absence of silverware on the sensor beds to control the flow of silverware sliding down the plate.

**Stage-02:** Following Akella's approach (2008), an inclined metering bin was placed at the end of the inclined plate to assist with further regulating and reducing batch size. The bin was constructed with dimensions 14"x9"x7", with one end enclosed and the other open so as to collect the silverware pieces that slide past the second electromagnet and reach the end of the downward inclined plate. The distance from the end of the inclined plate to the surface of the metering bin was made larger than the length of the knife, which is the longest silverware piece. A solenoid [Magnetic Sensor Systems #S-25-125-26-H] of 2.5" stroke length was placed under the bin, to pulse the base near the closed end. When the silverware pieces enter the metering bin they are sensed by proximity sensors beneath the bin and a signal then causes the solenoid to pulse the bin by striking the bottom, causing the bin to vibrate. This causes the pieces to move out through the open end of the bin onto the duck cloth.

As Akella (2008) described, further singulation is performed through permanent hemispherical magnets mounted on a leather belt, which is a continuous strip traversing two pulleys, one of which was driven by a variable speed electrical motor. The hemispherical magnets were glued to the top of the belt 10" apart. Duck cloth was placed above the belt such that silverware pieces attracted by a magnet slid along the cloth. An attempt was made to substitute wire screen cloth for the duck cloth and later with the combination of Teflon sheet and duck cloth. Section 2.6 describes the tests performed with these materials.

## **2.4 Design of Conveyor Feed Bin**

### **2.4 .1 Speed and Torque calculations of Conveyor**

As discussed in the Section 2.3, the vibrating feed bin used by Akella (2008) was replaced by a slow-moving conveyor. The conveyor was found to produce a more continuous flow of silverware to the downward inclined plate, and the variable speed drive of the conveyor allowed experimentation to find the best speeds. Before we selected the components of the conveyor, the speed and torque required to drive the conveyor had to be determined.

#### **Speed of the Conveyor**

Following Akella (2008), the size of the silverware batch was selected to be 400 pieces of silverware, composed of 100 pieces each of spoons, soup spoons, forks, and knives. Table 2.1 (Akella, 2008) provides the weight of each type of silverware:

Sl. No.	Type of Silverware	Weight (oz.)
1	Knife	2.7
2	Spoon	1.3
3	Soup Spoon	1.3
4	Fork	1.4

**Table 2.1: Weight of each type of silverware**

Thus, the total weight of the silverware batch  $W_{SL}$  is given by:

$$W_{SL} = 100(2.7 + 1.3 + 1.3 + 1.4) = 670 \text{ oz}$$

$$W_{SL} \approx 42 \text{ lb} \quad (1)$$

The conveyor's dimension had to be selected to mesh with the rest of Akella's machine (2008).

The overall width and length of this machine were 11¼" and 50", respectively, such that the

dimensions of our new belt conveyor were selected as 10" wide and 48" long. By

experimentation, we selected the maximum height of the silverware batch, distributed on the

conveyor, as 3", such that the dimensions of the silverware batch spread on the conveyor was

48"x10"x3", yielding 1440 inch<sup>3</sup>. Therefore, the volume occupied by a single silverware piece

was  $\frac{1440 \text{ inch}^3}{400 \text{ pieces}}$ , or 3.6 inch<sup>3</sup>/piece.

To achieve a singulation rate of 35 pieces/minute (minimum target set for this project), the

entire batch of 400 pieces would require 11.4 minutes to singulate, which yields a batch

singulation rate,  $R_B$  of:

$$R_B = \frac{1440 \text{ inch}^3 / \text{batch}}{11.42 \text{ min} / \text{batch}} = 126.09 \text{ inch}^3 / \text{min} \quad (2)$$



Since the average cross sectional area,  $A_B$ , of the batch was:

$$A_B = 10" \times 3" = 30 \text{ inch}^2, \quad (3)$$

the speed of conveyor,  $S_C$ , could be determined by:

$$S_C = \frac{R_B}{A_B} = \frac{126.09 \text{ inch}^3/\text{min}}{30 \text{ inch}^2} = 4.2 \frac{\text{inch}}{\text{min}} = 0.07 \text{ inch/sec} \quad (4)$$

### **Torque Required of Conveyor Drive Motor**

To determine the torque required of the motor driving the conveyor, we require conveyor speed, load on conveyor, friction of the conveyor belt on its supporting structure, and the diameter of driven conveyor roller. Based on the available geometry of the existing Akella machine (2008), we began with an assumed diameter of the driven roller of 1.5". Then, for the frictional force  $F_f$  acting on the fully loaded belt conveyor, we have:

$$F_f = W_{SL} \times C_f, \quad (5)$$

where,  $C_f$  is the coefficient of friction between the conveyor belt and the solid surface on which it slides. The Torque  $T_f$  required at the driven roller is then given by:

$$T_f = \frac{F_f \times D_r}{2 \times E_f} \times F_S \quad (6)$$

where,  $D_r$  is the driven roller diameter,  $E_f$  is the efficiency of the driven roller-belt interface and,  $F_S$  is the factor of safety to assure sufficient torque.

Then, combining (5) and (6), we obtain:

$$T_f = \frac{W_{SL} \times C_f \times D_r \times F_S}{2 \times E_f} \quad (7)$$

Initial measurements obtained by manually pulling a loaded belt over a smooth metal surface yielded  $C_f \approx 0.35$ . Then using  $W_{SL} = 42 \text{ lb}$ ,  $D_r = 1.5''$ ,  $F_S = 2.0$ , and  $E_f = 0.9$ , we obtain:

$$T_f = 392 \text{ oz} - \text{inch} \quad (8)$$

Accordingly we should size our conveyor roller to produce at least 392 oz.-inch at any speed within our belt speed range.

#### **2.4.2 Selection of Roller Shaft, Stepper Motor and Belts.**

##### **Stepper Motor**

After reviewing available belt roller electric motors, we selected a DC stepper motor because this could provide the needed torque at low speeds, with variable speed capability for experimental purposes. Based on the needed torque in (8), we found a DC stepper motor available in our lab whose output torque was 708 oz.-inch, which is almost twice the calculated torque. The specifications of this motor, shown in Fig. 2.1, are

- NEMA Size 34 Round Stepper Motor
- 1.8° Step Angle (200 steps per revolution)
- High Torque – Up to 700 oz. - inch
- Variable speed capability



**Fig 2.1 NEMA Size 34 Round Stepper Motor**

### **Stepper Motor Driver**

The DC stepper motor is controlled by a driver, and the pulse width calculation for the stepper driver is discussed in Chapter 3. From (4) the speed of the conveyor  $S_C$  (inch/sec) can be converted into the driven roller angular velocity  $N_d$  in RPM by:

$$N_d = \frac{S_C \times 60}{\pi \times D_r} \quad (9)$$

Then substituting  $S_C = 0.07 \text{ inch/sec}$  and  $D_r = 1.5 \text{ inch}$  in (8) yields, for the driven roller speed:

$$N_d = 0.89 \text{ RPM} \quad (10)$$

The driver for the stepper motor in Fig 2.1 was selected from Anaheim Automation, namely Microstep Driver MBC 12101, shown in Fig 2.2. This selection was made to match the 1.5 - 10.0 Amp current range of the motor, and has the following specifications:

- 2000 Steps per Revolution
- Operates from a DC Voltage of 20-80 Volts

- Directional Control
- Can receive clock signals at frequencies up to 100 KHz



**Fig 2.2 MBC 12101 Microstep Driver**

Clearly the driver can provide ten times more steps per revolution than the motor itself, but this is not problematical.

### **Driven and Follower Rollers**

Based on the assumed driven roller diameter of 1.5", a pair of the closest available conveyor rollers were purchased from McMaster-Carr. These conveyor rollers were designed for washdown applications and can resist corrosive environments. Specifications are:

- Length of conveyor roller – 10 inch
- Diameter of conveyor roller - 1.625 inch
- Capacity of conveyor roller - 100 lb.

The shaft of the driven roller was then machined to mate with the shaft of the stepper motor, whose diameter and length are 0.345" and 1.18", respectively.

Along with bearings, shaft couplings, and shaft collars the stepper motor and the driver shaft were assembled as shown in Fig 2.3

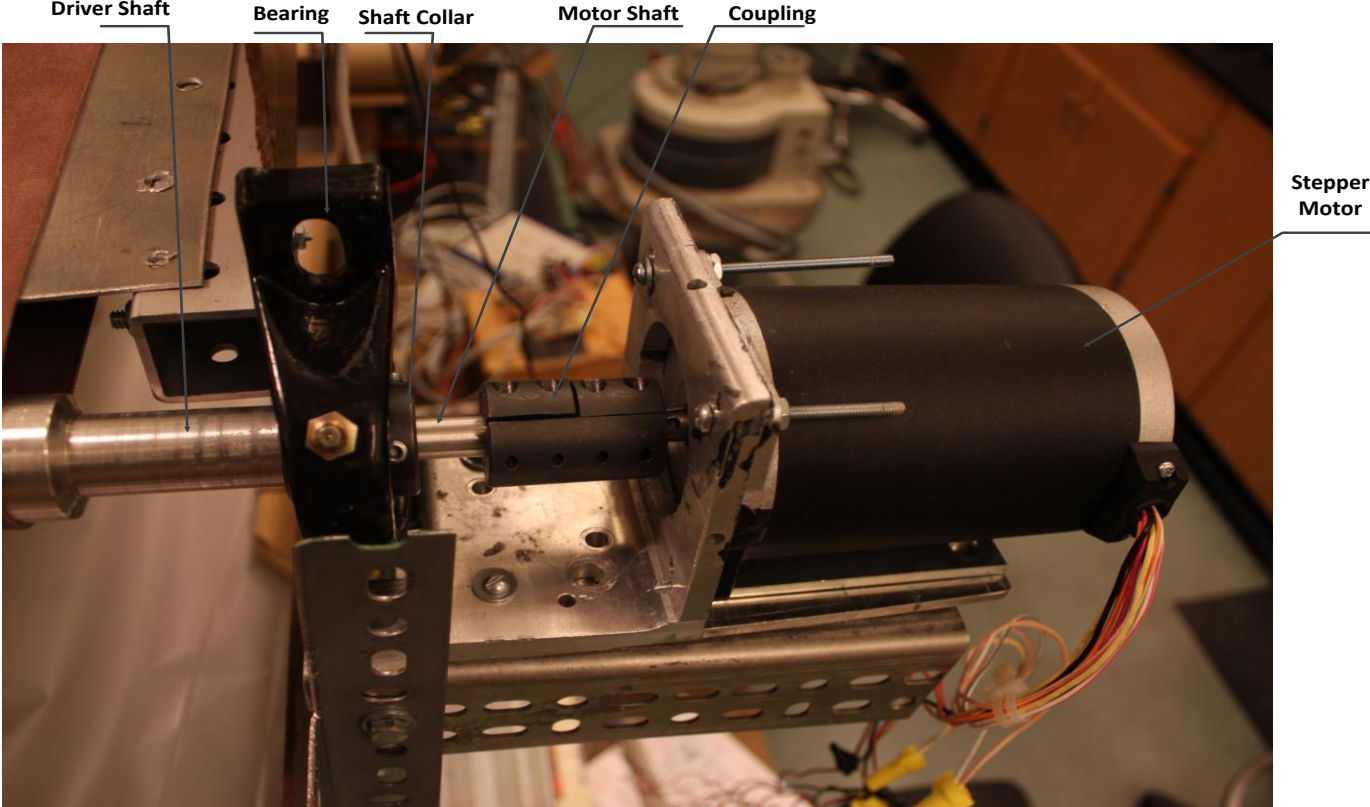


**Fig 2.3 Stepper Motor and Driver Shaft Assembly**

## Conveyor Belt

After investigating belt materials, we selected neoprene over PVC, nylon, elastomer and styrene butadiene rubber because of the following advantages of neoprene:

- Resistance to oil and moisture
- Minimal stretch and shrinking
- More flexible than PVC belting
- Friction surfaces on both sides, which would allow the belt to be reversed inside out if needed

In order to match the existing Akella machine (2008), a belt width of 8" was chosen, and a total length of 100" allowed approximately a 50" conveyor span between driven and follower rollers, which matched the overall length of the Akella machine (2008). The belt was purchased as an "endless" belt and connected through belt lacing. A belt thickness of 0.06" was deemed appropriate, for which hammer-in alligator lacing was chosen, shown in Fig. 2.4.

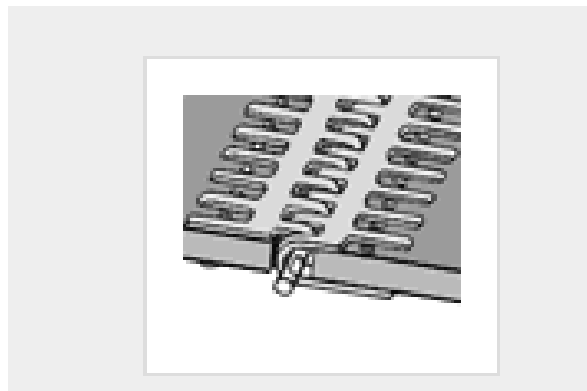


**Fig 2.4 Hammer-In Alligator Lacing**

## **2.5 Selection of Silverware Sensors**

Silverware sensors are required to indicate the presence of silverware at 3 locations:

- 1) Upper part of masonite downward inclined plate
- 2) Lower part of masonite downward inclined plate
- 3) Metering bin

The copper strip sensors used by Akella (2008) were able to reliably detect the presence of silverware, but they wore out quickly as more and more silverware passed over them.

Accordingly, one of the goals of the project herein was to find appropriate non-contact sensors to replace Akella's copper strip sensors (2008).

### **2.5.1 Investigation of Non – Contact Sensors**

We first investigated infra-red sensors, which operate by sending a beam of IR Light that can be blocked by an object passing through the beam, illustrated in Fig.2.5. When the beam is interrupted, the IR Receiver can signal such interruption, detecting the presence of silverware.

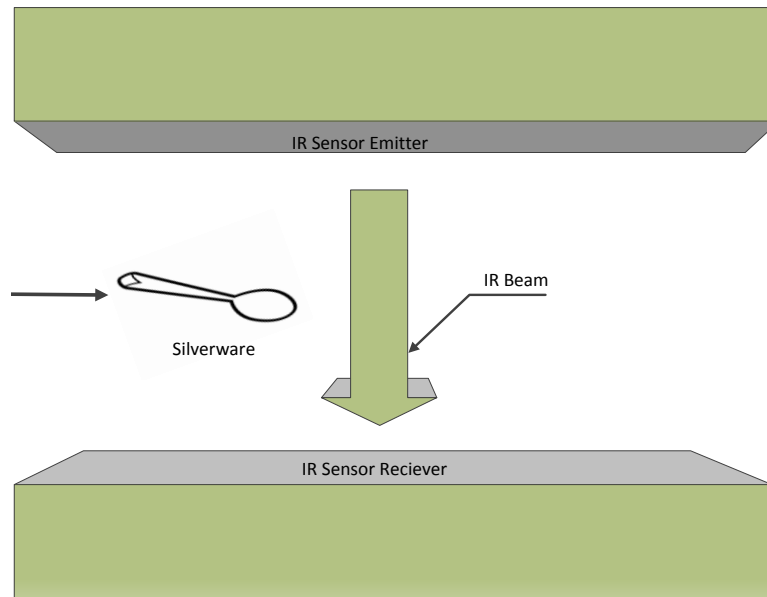


**Fig 2.5 IR Sensor Operation**

#### Advantages of IR sensors

- Sensors are small and easy to install
- Low power requirements; generally +5v is sufficient to power these sensors
- Fast response time, TM18 EZ-BEAM DC from Banner Engineering requires 1.5 ms for switching ON and 0.75ms for switching OFF
- Longer detecting distance, varies from 10 cm to 80 cm

#### Disadvantages of IR Sensors

- Provides unreliable detection of silverware due to the geometry of spoons and soup spoons, similar to the problems with photo-electric diode pairs discussed below
- Sensitive to atmospheric conditions such as moisture, leading to faulty signals



We also investigated a photo-electric diode pairs, which consist of an emitter transmitting a light beam and a receiver, with operation similar to the IR sensors in Fig. 2.5, to detect the presence of an object between them. Similar to the IR sensor, the emitter and receiver would be placed on either side of the masonite downward inclined plate. As a silverware piece passes down the inclined plate, the photo electrode diode receiver triggers a “high” if an object obstructs the beam. While the photoelectric diode pair worked well if the sliding object completely blocked the beam, Akella (2008) found that the curvature of spoons and soup spoons was such that the beam passed under or over them and did not trigger a “high”. Accordingly this type of sensor was not considered further.

A third type of sensor we investigated would use camera images, called an image sensor. The camera would continuously take images of the inclined plate area of interest, such that anytime silverware pieces appeared in an image, image software would detect this and provide a “presence” signal. Quality image sensors and their associated computer hardware are expensive, and we would require three such sensors. Moreover, the image processing software could be time consuming, which would affect the performance of the machine. Accordingly, we elected not to pursue them further.

Finally, we considered inductive proximity sensors used to detect the presence of metal objects. Such sensors operate using an oscillating electromagnetic field, such that metal objects passing through this field create a field disruption causing a damping current in the sensor circuit that indicates presence of a metal object. Because proximity sensors seemed to offer

numerous advantages with few disadvantages, we investigate them in some detail in the next section.

## **2.5.2 Investigation of Inductive Proximity Sensors**

### **Construction of an Inductive Proximity Sensor**

There are four basic components of an inductive proximity sensor: the sensor coil, the oscillator, the detector circuit and the output circuit, illustrated in Fig. 2.6

The sensor coil is a coil of copper wire tightly wound around a ferrite core located at the sensor face indicated in Fig. 2.6

The oscillator circuit generates a fluctuating current through the copper wire and induces a magnetic field in the coil. This field extends outwards from the sensor face, roughly in a dome shape, which forms the field of target detection for the inductive proximity sensor.

When a metal target passes through the inductive proximity sensor's field of detection, eddy currents build up in the metallic target. These currents dampen the magnetic field, induced by the oscillator circuit of the sensor. The detector circuit monitors the magnetic field strength and triggers a "presence" from the output circuit when the magnetic field strength is dampened to a sufficient level. Fig. 2.6 illustrates the components of inductive proximity sensor:

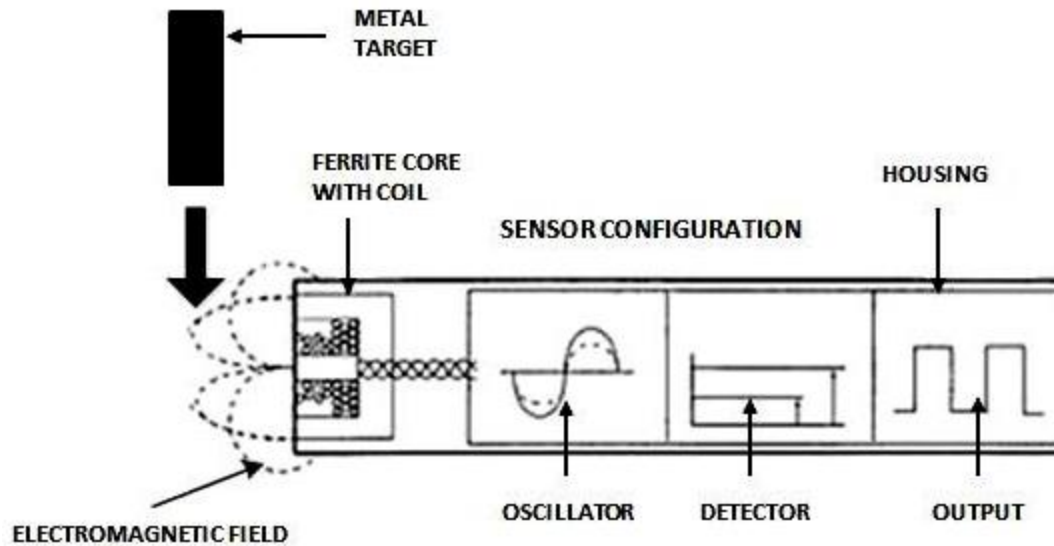


Fig 2.6 Components of Inductive Proximity Sensor, [1]

## Characteristics of an Inductive Proximity Sensor

### 1) Shape of Magnetic Field and Sensing Distance

As indicated in Fig. 2.7, the shape of the magnetic field of the inductive proximity sensor is roughly dome shaped, and the volume covered by the field depends on the diameter of the sensor and its sensing range. In Fig. 2.7 the distance “D” is the diameter of the sensing area and  $S_N$  is the sensing range. The solid lines (ON) in Fig. 2.7 represent the setting distance, and represent the distance from the sensor face to the position of the sensed object at which the inductive proximity sensor will trigger a positive output.

The dashed lines (OFF) in Fig. 2.7 represent the resetting distance, and represent the distance from the sensor face at which the inductive proximity sensor releases its output when the sensed object is removed from the field of detection.

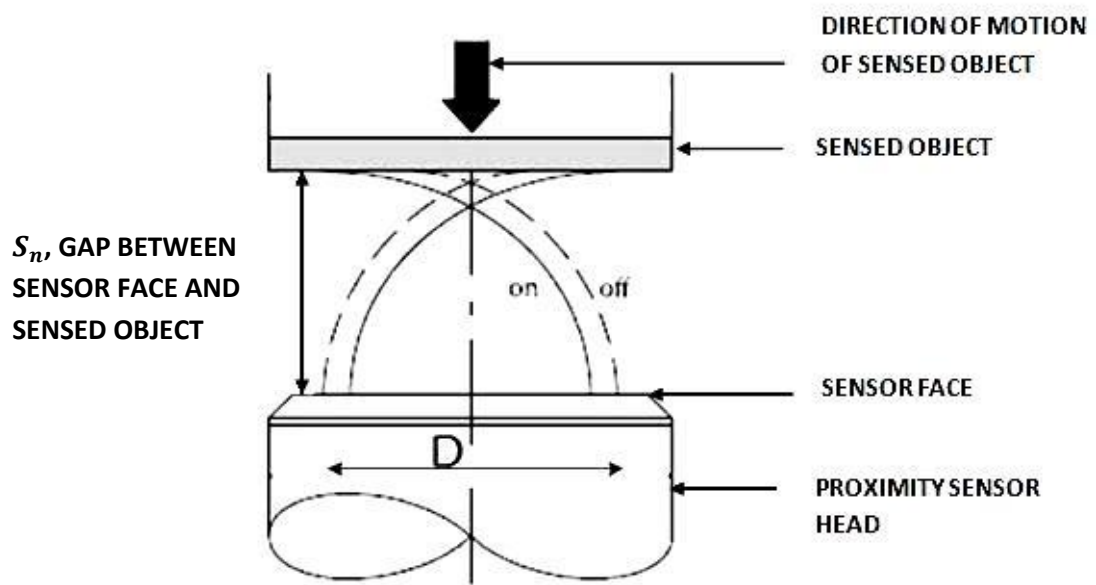


**Fig 2.7 Sensing Area Diagram of an Inductive Proximity Sensor, [2]**

Inductive proximity sensors can detect metal objects through nonmetallic barriers. To determine the sensing distance of materials other than mild steel, a correction factor must be applied, such that Nominal Sensing Range x Correction Factor = Actual Sensing Range. Table 2.2 gives the approximate correction factors for different materials:

<b>Target Material</b>	<b>Approximate Correction Factor</b>
<b>Mild Steel</b>	<b>1.00</b>
<b>Stainless Steel</b>	<b>0.85</b>
<b>Brass</b>	<b>0.50</b>
<b>Aluminum</b>	<b>0.45</b>
<b>Copper</b>	<b>0.40</b>

**Table 2.2 Correction Factors for different materials, [2]**

**2) Shielded/Flush and Unshielded/Non-Flush Proximity Sensors**

Inductive proximity sensors may be classified as either shielded or unshielded. Shielded proximity sensor construction includes a metal band that surrounds the ferrite core and coil arrangement, and therefore has the electromagnetic field concentrated directly in front of the sensing heads, as shown in Fig. 2.8. This type can be directly mounted into metal housings without causing false outputs. However the sensing distance is smaller than that of unshielded proximity sensors. Unshielded proximity sensors do not have a metal band in their construction, and therefore have a wide sensing angle, as shown in Fig. 2.8. They provide a longer sensing distance, but are easily affected by surrounding metals.

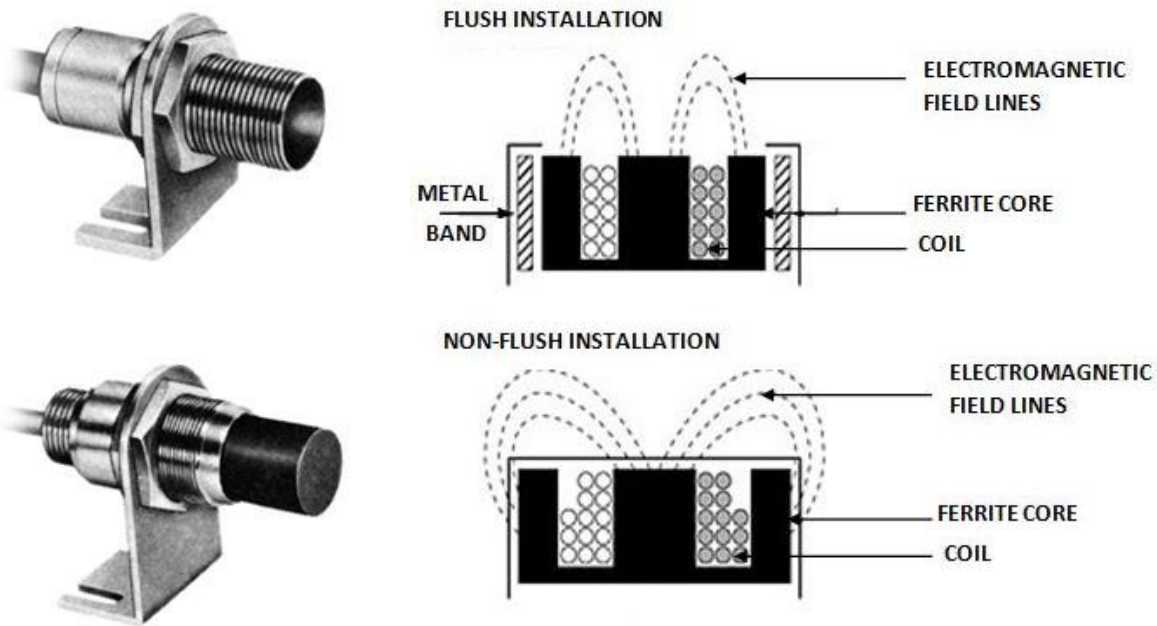


**Fig 2.8 Shielded (Top) and Unshielded (Bottom) Proximity Sensor with Their Magnetic Fields,**

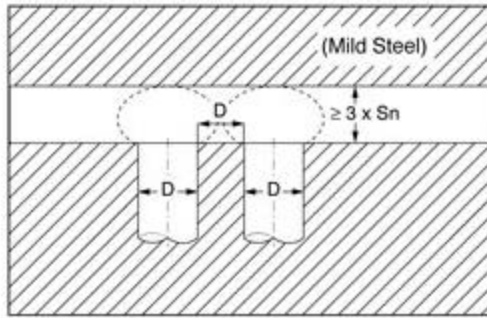
[1]

### 3) Mutual Interference

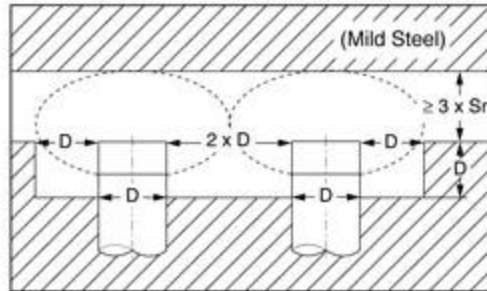
When proximity sensors are placed close to each other, the high frequency magnetic field created by one proximity sensor can affect the electromagnetism of the other, which can result in faulty outputs.

As indicated in Fig. 2.9, flush mount sensors placed side by side must be separated by a distance of at least one sensor diameter. Non-flush mount sensors must be separated by at least two sensor diameters. When sensors are placed opposing with each other, the separating distance must be greater than six times the sensing range, for both types of sensors.

Flush Mount Installation



Non-Flush Mount Installation



Opposing Installation

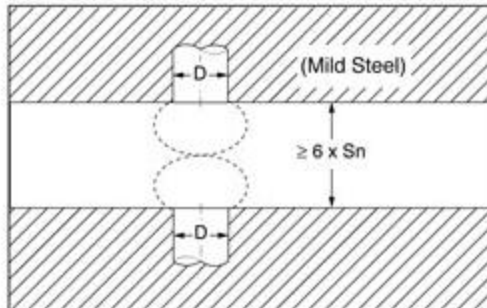


Fig 2.9 Mutual Interference of Inductive Proximity Sensors, [1]

#### **4) Input and Output of Inductive Proximity sensors**

Inductive proximity sensors available in the market are either AC or DC powered. The output from a proximity sensor is available in: normally open or normally closed, and NPN or PNP forms.

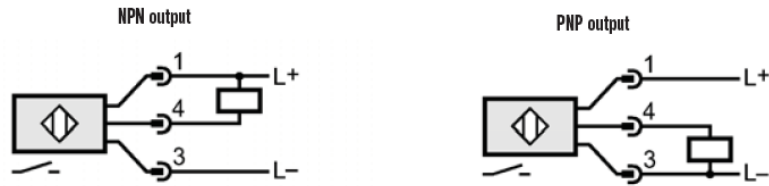
NO (normally open) output: The sensor output is initially at a “low” signal state when there is no metal target in the field of detection and sends a “high” signal when it detects a metal target.

NC (normally closed) output: The sensor output is initially at a “high” signal state when there is no metal target in the field of detection and sends a “low” signal when it detects a metal target.

NPN Output: The sensor has three terminals: positive, negative and common grounds, which correspond to Pin 1, Pin 3, and Pin 4, respectively, as shown in Fig. 2.10. NPN type sensors have their load connected between positive terminal and common ground. The “load” refers to the device the sensor powers, such as the microcontroller PIC 18f4520 in our application. The electrical input is connected to the negative terminal of the sensor.

PNP Output: PNP sensors have their load connected between the negative terminal and common ground. The electrical input is connected to the positive terminal of the sensor.





**Cable Assembly Wiring Colors:**  
**Pin 1 - Brown**  
**Pin 3 - Blue**  
**Pin 4 - Black**

**Fig 2.10 NPN and PNP Output, [2]**

### 5) Switching Frequency

The switching frequency is the maximum number of switching operations of a sensor per second. A switching operation includes sensing an object and resetting. The switching frequency of inductive proximity sensors varies from 300 Hz to 5000 Hz.

### Selection of an Inductive Proximity Sensor from Automation Direct

A variety of proximity sensors from different manufacturers were investigated. Based on our requirements, we selected the inductive proximity sensor PBT-AP-2H from Automation Direct.

The specifications that were considered important for our project were:

- Unshielded/ Non Flush Mount Type was selected because its sensing range is 15 mm, compared with only 10mm for the shielded/flush mount type.
- Automation Direct provides inductive proximity sensors with diameters of 3mm, 4mm, 8 mm, 12mm, 18 mm and 30 mm. To match Akella's (2008) sensor circuit which had a sensing area of 11.25"x6", we chose the sensor with the largest sensor diameter of 30

mm. The plan was to arrange a number of such sensors together in a sensor-bed to entirely cover Akella's sensing area (2008).

- The normally open (NO) type of inductive proximity sensors was selected because we desired a positive voltage signal sent to our microcontroller, PIC 18F4520, when a metal target is detected.

### **2.5.3 Design of Sensor-Bed**

As discussed in Section 1.3 Akella (2008) used three copper strip sensor circuits each having a sensing area of 11.25"x6". The challenge was to achieve a similar sensing area with the inductive proximity sensors. Before purchasing the PBT-AP-2H inductive proximity sensors, there were a several design considerations on the layout of the sensors:

- Sensors placed opposite each other

Fig. 2.11 depicts an initial design consideration of positioning sensor pairs within the wooden side walls on the inclined plate, opposing each other such that the sensor face was flush with the inner side of the wall. The figure shows Sensor 1 and Sensor 2 in the upper part of the inclined plate and Sensor 3 and Sensor 4 in the lower part. The sensing volume of an inductive proximity sensor is roughly dome shaped, as shown in the previous section, and the size of the dome depends on the diameter of the sensor and the sensing range, as shown in Fig. 2.7. Suppose we approximate the largest cross section of this dome with a rectangle, with width equal to the sensor face diameter and breadth equal to the sensing range. So a sensor with diameter 30 mm and sensing range of 50 mm will have an approximate sensing area of 30 mm x 50 mm.

The combined sensing areas of sensor 1 and sensor 2 would be used to detect the presence of silverware sliding down the inclined plate. The width of the downward plate is 235 mm, so the sensing range of each sensor must be at least 120 mm. However, one drawback of inductive proximity sensors is their low sensing range. Few sensors operate with a sensing range above 40 mm, and while there were a few available to provide 120 mm of sensing range, they were cost prohibitive.

Another drawback with this concept is the mutual interference of Sensor 1 with Sensor 2, and Sensor 3 with Sensor 4. For opposing installation of sensors, the sensors have to be separated by six times the sensing range as discussed in the previous section. If we consider the sensor with sensing range of 50 mm, they would be separated by 300 mm. However, the width of the Masonite sheet is only 235 mm. Hence this concept was discarded.

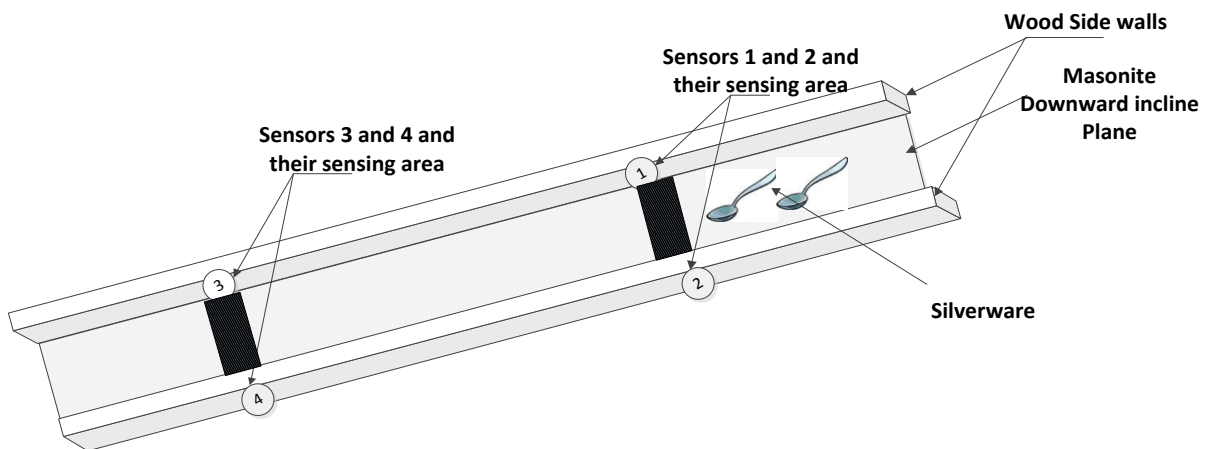


**Fig 2.11 Opposed positioning of sensors**

- Sensors placed side by side

We investigated placing the sensors side by side. In the opposed positioning concept, we required two sensors in each sensor-bed, but this concept will require more. As indicated above, the selected inductive proximity sensor PBT-AP-2H from Automation Direct selected for the design, whose diameter was 30 mm and sensing range was 15 mm.

The sensor-bed was constructed of 0.125" thick masonite sheet, 235 mm wide and 130 mm long, in order to span the sensing area of Akella (2008). Holes of 30 mm diameter were drilled in the Masonite sheet, as shown in Fig. 2.12, this arrangement was selected for two reasons:

1. To avoid the problem of sensor mutual interference
2. To cover the sliding area as completely as possible so that it would be improbable that a silverware piece sliding down the plate would not be detected.

Fig 2.13 is a photo of inductive proximity sensor, PBT-AP-2H. Mounting hex nuts that came with sensors were used to mount the sensors to the masonite sensor bed sheet. A clearance of 7.5 mm was included at the left and right edges of the sensor bed to avoid interference with the aluminum frames supporting the machine as shown in Fig.1.3. The mounted sensors on the masonite sensor bed are shown in Fig. 2.14.

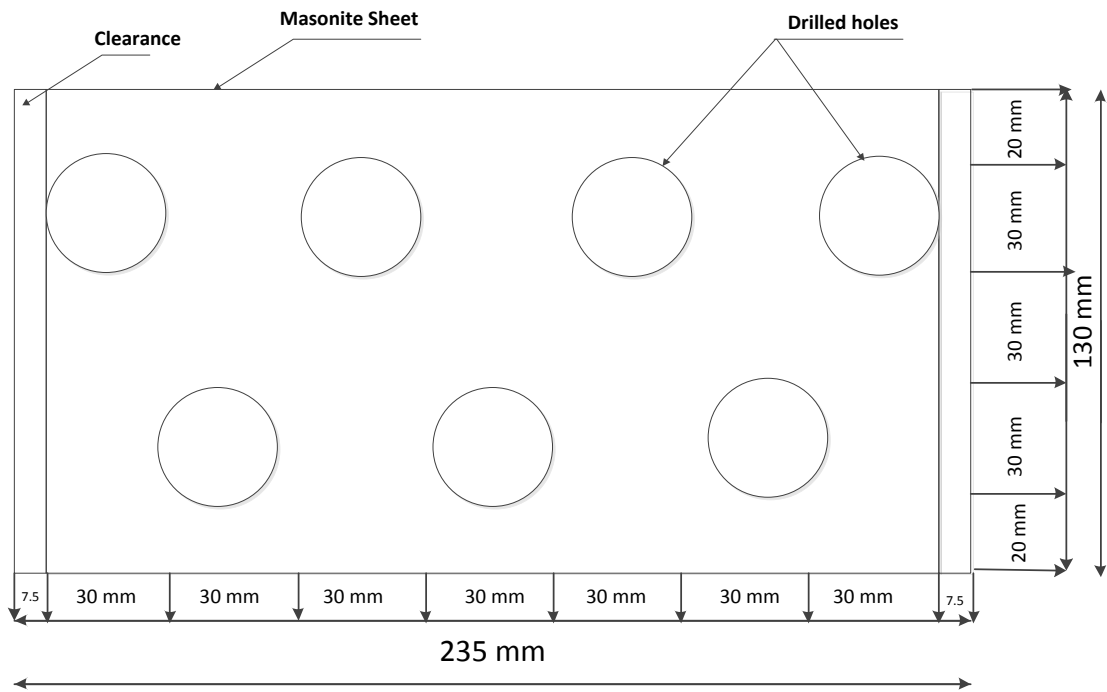


**Fig 2.12 Layout of Sensor Bed**



**Fig 2.13 Inductive Proximity Sensor PBT-AP-2H**

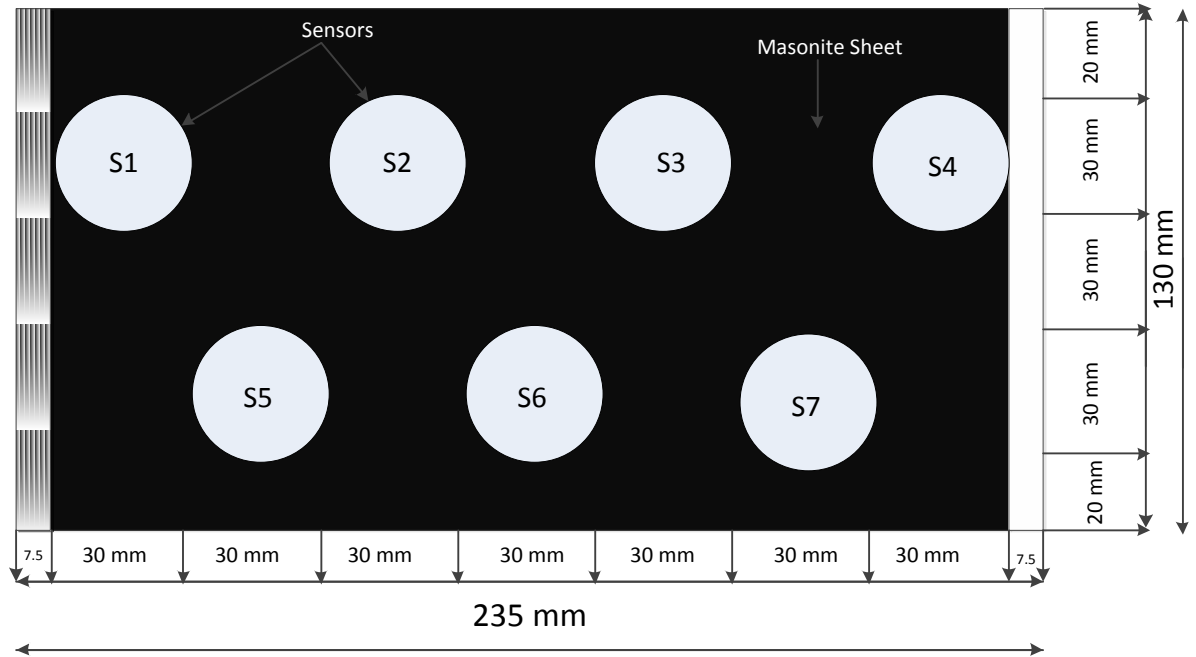


**Fig 2.14 Top View of Side by Side Positioning of Sensors in Sensor Bed**

**(S1, S2, etc. Indicate Different Sensors)**

The length of the sensors that protruded from the drilled holes of the sensor bed was selected such that they made contact with the underside of the Masonite downward inclined plate, as shown in Fig. 2.15.

There was a concern that placing the sensor-bed too close to the electromagnets might produce interference with the sensor electromagnetic fields. However, we found that if the nearest sensor to the electromagnets was at least one sensor diameter away from the nearest edge of electromagnets, no interference was detected.

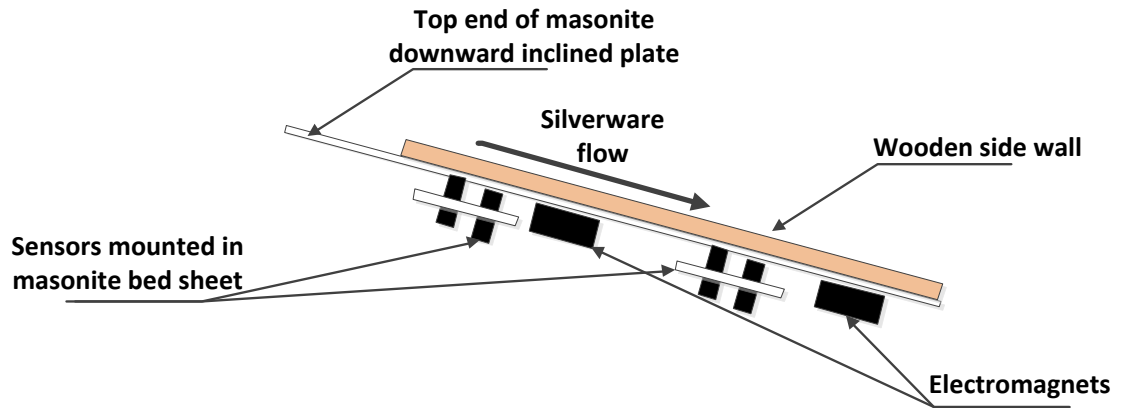


**Fig. 2.15 Side View of Masonite Downward Incline Plate, with Sensors and Electromagnets**

## **2.6 Selection of Material for Stage-02**

As depicted in Fig. 1.3, Stage 2 has supporting material covering a moving leather belt containing a series of hemispherical permanent magnets. Akella (2008) tried several different such materials to extract the best singulating performance. The friction between sliding silverware and the supporting material, the rigidity of the material, its magnetic permeability, and the cross-sectional thickness were some of the factors that influenced singulation performance. Akella (2008) investigated duck cloth, polypropylene 3/32" thick sheet, polypropylene 1/16" thick sheet, nylon 0.05" thick sheet, acrylic 0.06" thick sheet, polyethylene 1/16" thick sheet, teflon 1/32" thick sheet, cardboard sheet, and leather cloth. He found that duck cloth gave the best performance.

However, the duck cloth lacked durability, and we briefly investigated two other materials. The first of these was a 316 stainless steel wire cloths with mesh sizes 200 x 200 opening/inch and 150 x 150 openings/inch each ,having dimensions 18"x48". Since the wire cloth was constructed from 316 stainless steel, it was non-magnetic, such that hemispherical magnets on the moving belt would not be attracted to this cloth.

We started the trial run with the 150 x 150 mesh wire cloth. The belt drive was operated at 24 V because Akella (2008) achieved the best simulating performance with this setting, and 200 pieces of silverware were used for the trial run, with the total operating time for singulation of 8 minutes and 12 seconds. The singulation speed achieved was 24.39 pieces per minute, which was lower than that achieved by duck cloth.

When the second trial run was performed on the 150 x 150 mesh wire cloth, it became excessively worn and torn. A trial also was performed on the 200 x 200 mesh wire cloth, but it wore off during the first trial. The damaged cloths are shown in Fig. 2.16. We observed that the wire cloth appeared to offer excessive friction to the silverware flow, and hence wore out at a very rapid rate, much faster than the duck cloth used by Akella (2008).





**Fig 2.16 Damaged 150 x 150 (top) and 200 x 200 (bottom) Mesh Wire Cloth**

We also briefly investigated rubber tubing as a supporting material, but found that this produced poor singulation performance due to high friction between silverware pieces and the rubber.

Akella (2008) investigated using Teflon 1/32" sheet, with which he obtained good singulation performance due to its smooth surface and low friction between sheet and silverware. However, after substantive experimentation, the sheet became rigid and damaged in areas where silverware pieces dragged repeatedly. So, we decided to glue thin plastic sheet that was available in the lab to the middle portion of teflon sheet, where the silverware are dragged. The combination of thin plastic sheet and teflon sheet as shown in Fig. 2.17 offered a smooth surface and also substantially reduced surface wear. Trials were performed with a batch of 300 pieces of silverware at various belt speeds. The teflon sheet with plastic liner showed promising results which will be discussed in detail in Chapter 4.

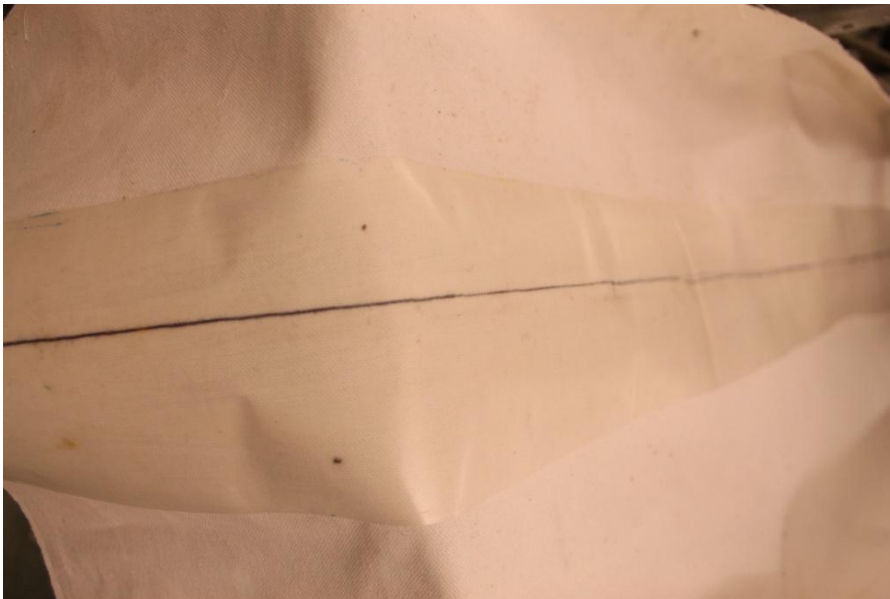


**Fig. 2.17 Combination of Plastic sheet with Teflon Cloth**

In this chapter, we discussed the electrically powered components and, selection and positioning of these components, that we considered for the silverware singulation machine. It is essential that these components communicate and coordinate with each other to achieve our silverware singulation goal. A complete sketch of the present set up is shown in Fig. 2.17. A microcontroller along with an intelligent algorithm to aid in achieving this goal will be discussed in the next chapter.

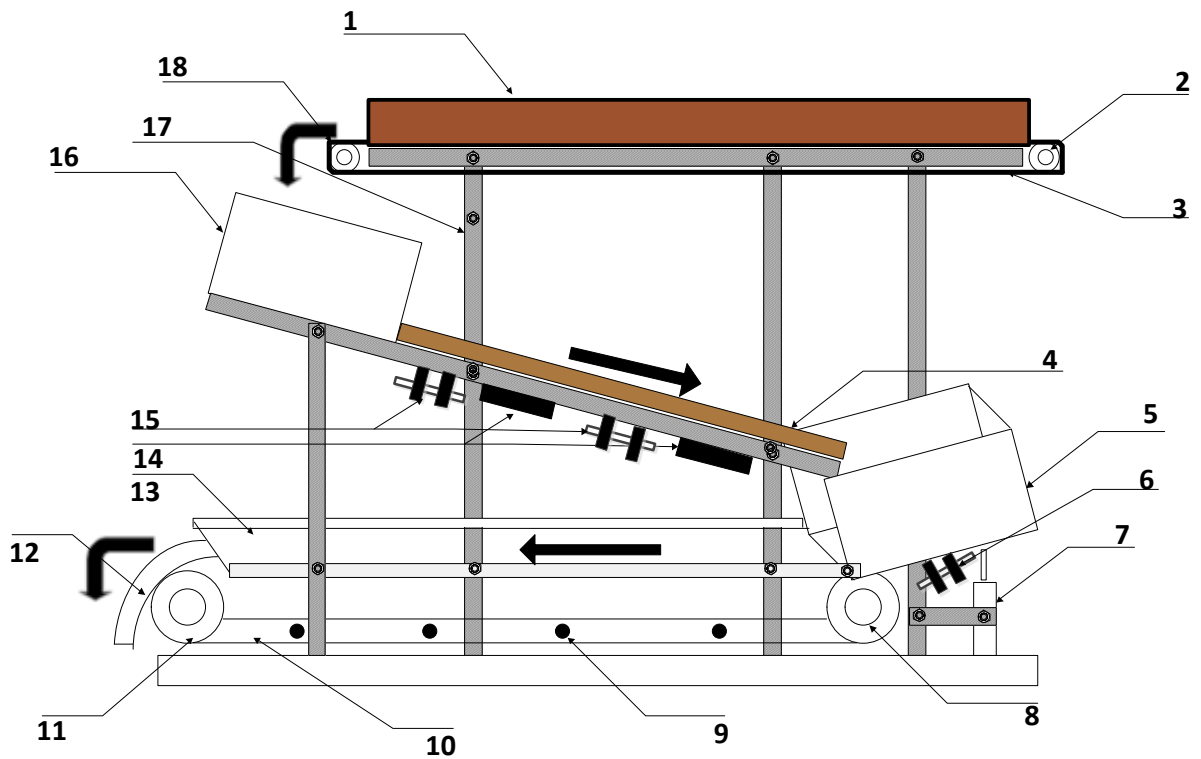


**Fig 2.18 Sketch of Present Setup**

**Bold arrows indicate silverware flow**

- |                                       |                                     |
|---------------------------------------|-------------------------------------|
| 1. Conveyor Wall                      | 2. Driven Roller for Conveyor       |
| 3. Neoprene Belt                      | 4. Masonite Downward Inclined Plate |
| 5. Metering Bin                       | 6. Sensor Bed -3                    |
| 7. Solenoid                           | 8. Driver Roller for Leather Belt   |
| 9. Hemispherical Magnets              | 10. Leather Belt                    |
| 11. Driven Roller for Leather Belt    | 12. Scrapper                        |
| 13. Plastic Lined Teflon Cloth        | 14. Electromagnets                  |
| 15. Sensor Bed - 1 and Sensor Bed - 2 | 16. Receiving Bin                   |
| 17. Driver Roller for Conveyor        | 18. Aluminum Frames                 |

## **CHAPTER 3**

### **DESIGN OF CONTROL SYSTEM**

Chapter 2 describes the various hardware components, and their positioning, that are used in the silverware singulating machine. A control system is needed through which these hardware components can communicate and be coordinated to obtain the desired goal. The hardware components in our machine may be classified as either input or output devices. Input devices in our machine are the three inductive proximity sensor beds placed on the downward inclined plate and the metering bin. Output devices are the DC stepper motor driving the conveyor, electromagnets, and the metering bin solenoid. We also require a microcontroller, which is a programmable input/output device that collects input from the sensors, analyses them, and sends commands to the output devices. This chapter describes:

- Speed Control of DC motor
- Coordination of proximity sensors with the DC stepper motor, the electromagnets, and the solenoid

### 3.1 Speed Control of DC Stepper Motor

DC Stepper motors are normally controlled by pulse width modulation, a method in which a series of digital pulses is used to control an analog circuit. The power delivered to the circuit is determined by the duration and frequency of the pulses, and could be provided by a timer such as the LM555 made by National Instruments, or by built-in timers in a microcontroller, such as the PIC 18F4520, which we had available. Because of ease of use, we elected to use the built-in timer in our microcontroller. A generic waveform output of a 5-Volt pulse timer is shown in Fig. 3.1.

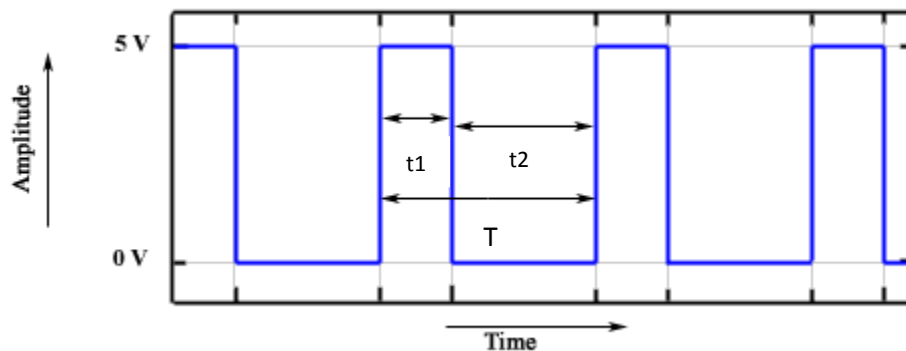


**Fig 3.1 Waveform Output of a Timer**

From the waveform output, the output “high” time is  $t_1$ , and the output “low” time is  $t_2$

The total time period,  $T$ , is thus:

$$T = t_1 + t_2 \quad (11)$$

The frequency of the pulse,  $F$ , is then given by:

$$F = \frac{1}{T} \quad (12)$$

From (10), the driven roller speed was  $N_d = 0.89 \text{ RPM}$ , such that the time taken for 1 revolution of the driven roller,  $T_R$  is given as:

$$T_R = \frac{1}{N_d} \quad (13)$$

From section 2.4.2, the stepper motor could achieve 2000 steps per revolution. The time taken for 1 step,  $T_S$  is then given by:

$$T_S = \frac{T_R \times 60}{2000} \quad (14)$$

Using  $N_d = 0.89 \text{ RPM}$  in (16), we obtain:

$$T_S = 0.035 \text{ sec} \quad (15)$$

The PIC 18F4520 has three timers: Timer\_0, Timer\_1 and Timer\_2. Timer\_0 and Timer\_2 operate in 8 bit mode, and Timer\_1 operates in 16 bit mode. In 8 bit mode, the timer counts from 0 to  $2^8$ , and in 16 bit mode it counts from 0 to  $2^{16}$ . To assure that the conveyor could move sufficiently slow, we decided to reduce the time period, T from 0.035 sec given in (15) to 0.01 sec.

From the specification sheet of the PIC 18f4520, we obtain its clock frequency,  $C_f$  as:

$$C_f = 20 \times 10^6 \text{ Hz} \quad (16)$$

Therefore, time taken for 1 clock cycle is given by,  $T_{CS}$  :

$$T_{CS} = \frac{1}{C_f} \quad (17)$$

Each statement (instruction) in the software code contributes to the calculation of the time period as well. The time taken to process 1 instruction,  $T_i$  is given as:

$$T_i = 4 \times T_{CS} \quad (18)$$

The .lst file created during software code compilation, shows that there were 22 statements generated for the Timer\_0 sub-code. The high time,  $t_1$  is the time required to execute these statements, and by using 17, and (18)  $t_1$ , is given by:

$$t_1 = \text{Number of statements in Timer sub code} \times \frac{4}{C_f} \quad (19)$$

Using  $C_f = 20 \times 10^6 \text{ Hz}$ , and *Number of statements in Timer sub code* =22, yields:

$$t_1 = 4.4 \text{ micro seconds} \quad (20)$$

Using  $T = 10.00 \text{ mili seconds}$ , and  $t_1 = 4.4 \text{ micro seconds}$  in (11) gives  $t_2$  as:

$$t_2 = (10 - 0.0044) \times 10^{-3} \text{secs} = 9.9956 \text{ mili seconds} \quad (21)$$

Therefore, the “high” time  $t_1$ , is primarily dependent on the number of statements in the software code. However, the “high” time can be increased by adding a delay statement in the timer sub-code. The delay statement suspends the execution of the next statement in the software code for a specified period of time. The “high” time must always be lower than the desired time period  $T$ , otherwise the software code would malfunction.



The time period, T for the timer circuits in the PIC 18f4520 is given as :

$$T = Num\_count \times P_S \times T_i \quad (22)$$

where, *Num\_count*, is a number to be counted in a timer. As Timer\_0 operates in 8 bit mode, it counts from 0 to 255 (256 numbers). However, the count can be reduced by changing the Starting Point from 0 to any number greater than 0, but less than 255. The purpose of reducing the count is to obtain lower time periods. Therefore, *Num\_count* is given by:

$$Num\_count = End\ Point - Starting\ Point \quad (23)$$

where, End Point is  $2^8$  for Timer\_0. In (22)  $P_S$  is a prescalar, or frequency divider, which enables further division of clock frequency. The division options for  $P_S$  are: 1/2, 1/4, 1/8, 1/16, 1/32, 1/64, 1/128, and 1/256

From (18), (22), and (23) the Starting Point is given by:

$$Starting\ Point = End\ Point - \frac{T \times C_f}{P_S \times 4} \quad (24)$$

Using  $C_f = 20 \times 10^6\ Hz$ ,  $T = 0.01\ sec$ ,  $P_S = 1/256$ ,  $End\ Point = 2^8$  yields:

$$Starting\ Point = 61 \quad (25)$$

The Timer\_0 now counts from 61 to 255 instead of 0 to 255 thus resulting in a time period of 0.01 Hz. The time period can be easily varied by changing the values of starting point and prescalar in the software code.

### **3.2 Description of the Hardware and Software.**

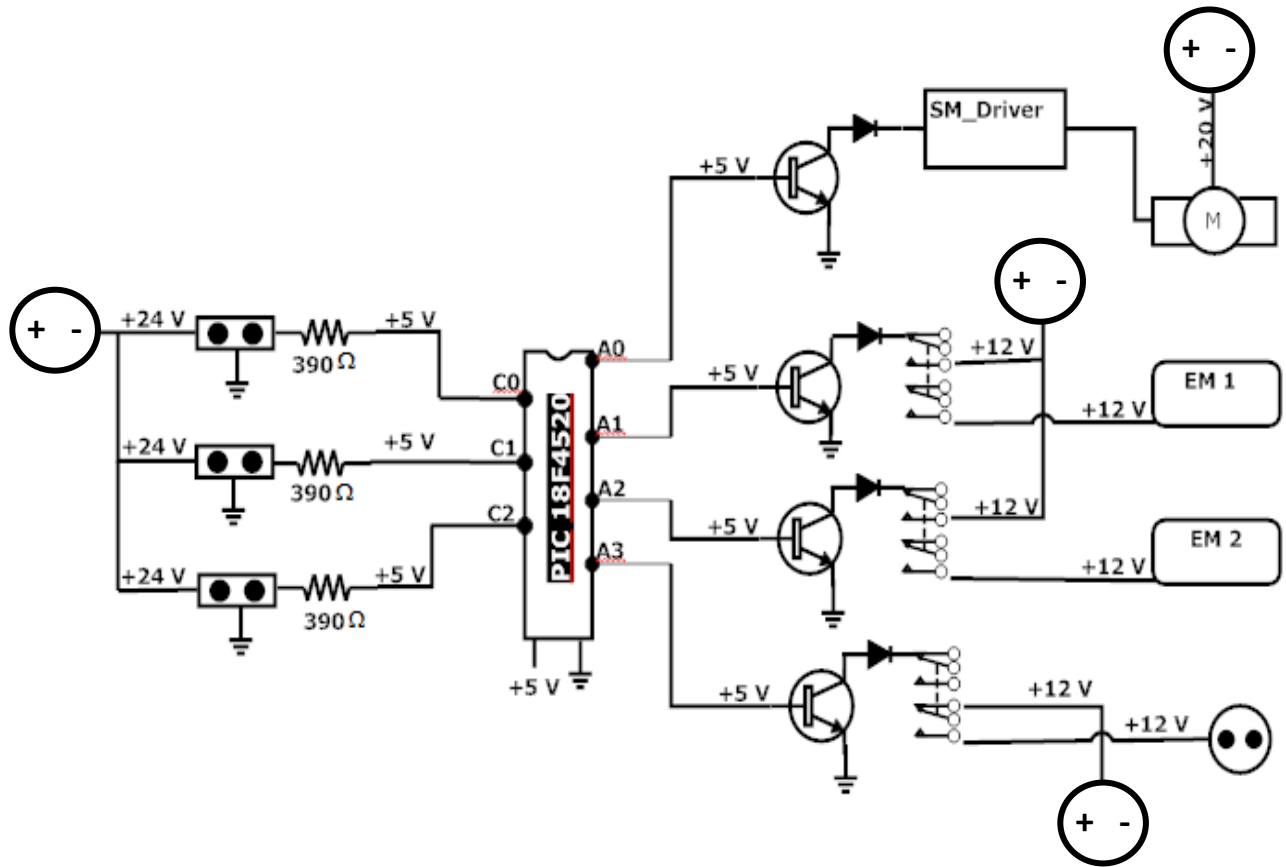
The microcontroller PIC 18f4520 was selected as the CPU to interact with the sensors and all the actuators in the silverware singulating machine. The PIC 18f4520 is a 16 bit, 44 pin microcontroller that offers a C compiler. Through the C compiler, we generate the .hex files for the software code written in C language. Another advantage of this PIC is its flash memory, through which the software code can be electrically erased any number of times and reprogrammed. Fig.3.2 presents a circuit diagram showing all the signal and power connections.

The input pins of the microcontroller are connected to the three sensor beds, and the output pins are connected to the actuators: the upper and lower electromagnets, the stepper conveyor motor and the metering bin solenoid. A voltage of +24 V was supplied to the inductive proximity sensors from a 0-30 V variable DC power supply available in our lab. The sensor output was approximately +24V, which was passed through appropriate resistors to reduce the voltage to +5V, because the microcontroller's operating voltage is 2.0 to 5V.

The microcontroller collects the output from each sensor bed, analyses them based on the algorithm described in Section 3.3, and sends corresponding signals toward the appropriate devices. However, signals are not directly sent to the actuators, but are initially sent to IRF 510 MOSFET transistors for switching electronic signals. The voltage signal output from the microcontroller is +5V, but the actuators require higher voltage for operation. DPDT (Double Pole Double Throw) Relays, used by Akella (2008) were used as the switching and amplifying devices. They are used to interface an electrical circuit, which operates at a low voltage, to an electrical circuit which operates at a high voltage. In our case the IRF 510 transistors operating

at +5V were the low voltage electrical circuit, and the +12V power supplies were the high voltage electrical circuits. Thus, these relays turn on the actuators, namely the upper and lower electromagnets, and the solenoid. However, for the stepper motor, the voltage signal for the MOSFET transistor is sent to the stepper motor driver, which controls the stepper motor powered by a +20V power supply.

Switching mode power supplies (SMPS) were borrowed from the MAE Electronics Lab to be used as power supplies for the electromagnets and the solenoid. They could be operated at either 6V or 12 V, but to assure adequate power we chose 12 V to power the electromagnets and the solenoid. A 0-30 V variable DC power supply was used to drive the belt motor of Stage - 02 at different speeds in order to test the belt at different speeds for singulating efficiency and throughput. However, the motor was not connected to the microcontroller, but instead was manually switched on and off at the beginning and end of each experiment, respectively.










 -POWER SOURCE	 - DIODE
 -SENSOR BED	SM_DRIVER - STEPPER MOTOR DRIVER
 -RESISTOR	 -DPDT RELAY
C0, C1, and C2 - INPUT PINS	EM1 - UPPER ELECTROMAGNET
A0, A1, A2, and A3 – OUTPUT PINS	EM2 - LOWER ELECTROMAGNET
 -IRF 510 MOSFET TRANSISTOR	 - SOLENOID

Fig. 3.2 Circuit Diagram for the Silverware Singulation Set up

### 3.3 Coordination of Sensors, Stepper Motor, Electromagnets and Solenoid

There are 3 sensor beds located as shown in Fig. 1.3: two below the downward inclined plate and one below the metering bin. There are two electromagnets below the inclined plane and a solenoid below the metering bin. For microcontroller output signals, the initial status of the stepper motor and the solenoid will be set to “low”, while the electromagnets will be set to “high”, before the start of the experiment. The sensor bed statuses are checked at a frequency of 10 Hz. Timer\_1, which operates in 16 bit mode, is employed to check the status. The time between sensor bed checks required from Timer\_1 is thus 0.1 sec. The Timer\_1 sub-code in the .lst file shows there are 330 statements generated.

Using  $C_f = 20 \times 10^6 \text{ Hz}$ , and *Number of statements in Timer sub code* =330, in (19) gives  $t_1$  as:

$$t_1 = 0.66 \text{ micro seconds} \quad (26)$$

Using  $T = 0.1 \text{ seconds}$ , and  $t_1 = 0.66 \text{ micro seconds}$  in (11) gives  $t_2$  as:

$$t_2 = 99.93 \text{ mili seconds} \quad (27)$$

The sensor bed check interval of 0.1 sec was achieved by using  $C_f = 20 \times 10^6 \text{ Hz}$ ,  $T = 0.1 \text{ sec}$ ,  $P_s = 1/256$ , and *End Point* =  $2^{256}$  in (24), to obtain

$$\text{Starting Point} = 3036 \quad (28)$$

Timer\_1 now counts from 3036 to  $2^{16}$  instead of 0 to  $2^{16}$ , which results in a time period of 0.1 sec.

Akella's parallel approach (2008) was employed, in which the action sequence for each actuator is defined by a truth table for the three sensor beds. The presence of 3 sensors resulted in 8 ( $2^3$ ) possible configurations. Timer\_1 checks the statuses of the sensors every 0.1 sec. Based on the status for each signal configuration, an intelligent action sequence is defined in our software code. As the code is interrupted every 0.1 sec, the algorithm selects the appropriate action sequence based on the latest sensor status. Our truth table is given by Table 3.1

Sensor Bed 1	Sensor Bed 2	Sensor Bed 3	Stepper Motor	Upper Electromagnet	Lower Electromagnet	Solenoid
0	0	0	1	0	0	0
0	0	1	1	0	1	1
0	1	0	1	1	0	0
0	1	1	1	1	1	1
1	0	0	0	0	0	0
1	0	1	0	0	1	1
1	1	0	0	1	0	0
1	1	1	0	1	1	1

**Table 3.1 Truth Table for Sensor Configuration, Akella (2008)**

"0" for Table 3.1, Sensor Bed 1, Sensor Bed 2, and Sensor Bed 3 columns represents the absence of silverware on the sensor beds, and "1" represents the presence of silverware. "0"

for the Stepper Motor, Upper Electromagnet, Lower Electromagnet and Solenoid columns represents the OFF position, and "1" represents the ON position.

A summary of the conditions to control the actuators is as follows:

- Conditions to control the stepper motor: The stepper motor is turned on if there is no silverware detected by either Sensor Bed 1 or Sensor Bed 2; it is turned off if there is silverware present on either Sensor Bed 1 or Sensor Bed 2.
- Conditions to control the electromagnets: Electromagnet 1 (Upper Electromagnet) is turned on if Sensor Bed 2 detects silverware; otherwise it is turned off. Electromagnet 2 (Lower Electromagnet) is turned on if Sensor Bed 3 detects silverware; otherwise it is turned off.
- Conditions to control the solenoid: The metering bin solenoid is turned on if Sensor Bed 3 detects silverware; otherwise it is turned off.

Using the singulation system described in Chapter 2 and 3, experiments were performed, and the results are presented in Chapter 4.

## **CHAPTER 4**

### **EXPERIMENTAL RESULTS**

After implementing the design and software described in the previous chapters, the silverware singulating machine was ready for recording results. The primary indicators of performance, computed from the recorded results, are singulating efficiency and throughput. Singulating efficiency is the percent of singulated individual pieces of silverware that the test rig produced from a mixed batch placed in the conveyor feed bin at the start of the run. Throughput is defined as the number of singulated individual pieces produced in a single test run divided by the total time in minutes of the test run. The following six variables, as used by Akella, (2008), were recorded for each test run.

1. Number of individual pieces dispensed
2. Number of sets of 2 pieces dispensed at the same time
3. Number of sets of 3 pieces dispensed at the same time
4. Number of groups of larger than 3 pieces dispensed at the same time
5. Number of silverware pieces not dispensed from the rig at the end
6. Total time taken



For the purpose of clarity and understanding, presentation and discussion of the results have been sub-divided into five sections. Section 4.1 contains test results for singulating efficiency and throughput, Section 4.2 contains test results for singulating efficiency and throughput without the use of Sensor Bed-1, Sensor Bed -2 and electromagnets. A list of testing conditions is given below:

1. The operating speed of the conveyor feed bin was 0.07 inch/sec, for which the stepper motor driving the conveyor feed bin received a constant voltage of 14.6V DC. The silverware spread on the conveyor feed bin was kept at a height of 4", close to the maximum height that could be accommodated.
2. The downward inclined plate was set at an angle of 20.7° below horizontal, with its surface lined by a thin plastic sheet, to reduce friction so that the silverware pieces could more easily slide down the incline.
3. As used by Akella, (2008), both DC electromagnets were operated at 5V DC input, which generated sufficient magnetic field to meet the requirements of this experiment.
4. As in the experiments performed by Akella, (2008), the hemispherical-magnet belt driver motor was operated at 18V, 21V, 24V, and 27V to determine the effect of belt speed on singulating performance. The passing rate of these magnets at these voltages was 52, 59, 67, and 76 magnets/min, respectively, with the magnets nominally spaced 10 inches apart on the belt.

#### 4.1a Singulating Efficiency Results at Various Belt Speeds

In tables 4.1 through 4.4, and 4.9 through 4.11, the headers for the columns titled “Number of Pieces in Twos”, “Number of Pieces in Threes”, and “Number of Pieces in Groups” represent the final numerical values obtained by multiplying the actual experimental numbers with their corresponding multipliers. For example, in Table 4.1, in the first row and the 3<sup>rd</sup>, 4<sup>th</sup>, and 5<sup>th</sup> columns from the left, 22 represents the eleven sets of 2 pieces, 9 represents three sets of 3 pieces, and 0 represents no sets of 4 or more pieces.

Case 1: Magnet rate of 52 magnets/min

Run No.	Total Number of Silverware Pieces	Number of Pieces in Twos	Number of Pieces in Threes	Number of Pieces in Groups	Number of Pieces Left Over	Number of Singulated Pieces	Singulating Efficiency %
1	400	22	9	0	3	366	91.5
2	400	28	3	0	3	366	91.5
3	400	24	3	0	5	368	92
4	400	22	6	0	0	372	93
Avg.	400	24	5.25	0	2.75	368	92

**Table 4.1 – Singulating Results for Magnet Rate of 52 magnets/min**

Case 2: Magnet rate of 59 magnets/min

Run No.	Total Number of Silverware Pieces	Number of Pieces in Twos	Number of Pieces in Threes	Number of Pieces in Groups	Number of Pieces Left Over	Number of Singulated Pieces	Singulating Efficiency %
1	400	22	6	0	2	370	92.5
2	400	26	0	0	0	374	93.5
3	400	28	0	0	3	369	92.25
4	400	16	3	0	2	379	94.75
Avg.	400	23	2.25	0	1.75	373	93.25

**Table 4.2 – Singulating Results for Magnet Rate of 59 magnets/min**

Case 3: Magnet rate of 67 magnets/min

Run No.	Total Number of Silverware Pieces	Number of Pieces in Twos	Number of Pieces in Threes	Number of Pieces in Groups	Number of Pieces Left Over	Number of Singulated Pieces	Singulating Efficiency %
1	400	16	0	0	0	384	96
2	400	12	0	0	4	384	96
3	400	12	0	0	1	387	96.75
4	400	18	0	0	2	380	95
Avg.	400	14.5	0	0	1.75	383.75	95.94

**Table 4.3 – Singulating Results for Magnet Rate of 67 magnets/min**

Case 4: Magnet rate of 76 magnets/min

Run No.	Total Number of Silverware Pieces	Number of Pieces in Twos	Number of Pieces in Threes	Number of Pieces in Groups	Number of Pieces Left Over	Number of Singulated Pieces	Singulating Efficiency %
1	400	14	0	0	2	384	96
2	400	14	0	0	0	386	96.5
3	400	10	0	0	1	389	97.25
4	400	12	0	0	5	383	95.75
Avg.	400	12.5	0	0	2	385.5	96.38

**Table 4.4 – Singulating Results for Magnet Rate of 76 magnets/min**

As can be seen from tables 4.1 – 4.4, four test runs were performed for each different magnet rate. The singulating efficiency varied from 91.5% to 97.25% for individual test runs, over all magnet rates. For each magnet rate, averages were computed over the four test runs and presented in the last row of each table. The average singulating efficiency varied from 92% to 96.38%. The overall average efficiency for all the test runs at all magnet rates was 94.4%.

Comparing with Akella's results (2008), whose singulating efficiency varied from 89.25% to 94.68% for individual runs, over all magnet rates, average singulating efficiency varied from 90.33% to 94.96%, and the overall average efficiency for all the test runs was 92.9% we observe a 1.5% increase in the overall average singulating efficiency in the current apparatus.

#### 4.1b Throughput Results at Various Magnet Rates

In tables 4.5 – 4.8, the run numbers indicate the corresponding runs in tables 4.1 – 4.4. This is indicated by the results in the 3<sup>rd</sup> column from the left in tables 4.5 – 4.8 being the same as the results in the seventh column from the left in tables 4.1 – 4.4 for the same magnet rates.

Case 1: Magnet rate of 52 magnets/min

Run No.	Number of Singulated Pieces	Total Time Taken (secs)	Number of Singulated Pieces/Min
1	366	748	29.35
2	366	712	30.84
3	368	755	29.24
4	372	734	30.40
Avg.	368	737.25	29.96

**Table 4.5 - Singulating Throughput for Magnet Rate of 52 magnets/min**

Case 2: Magnet rate of 59 magnets/min

Run No.	Number of Singulated Pieces	Total Time Taken (secs)	Number of Singulated Pieces/Min
1	370	689	32.22
2	374	712	31.51
3	369	698	31.71
4	379	721	31.53
Avg.	373	705	31.74

**Table 4.6 - Singulating Throughput for Magnet Rate of 59 magnets/min**

Case 3: Magnet rate of 67 magnets/min

Run No.	Number of Singulated Pieces	Total Time Taken (secs)	Number of Singulated Pieces/Min
1	384	619	37.22
2	384	625	36.86
3	387	598	38.82
4	380	607	37.56
Avg.	383.75	612.25	37.61

**Table 4.7 - Singulating Throughput for Magnet Rate of 67 magnets/min**

Case 4: Magnet rate of 76 magnets/min

Run No.	Number of Singulated Pieces	Total Time Taken (secs)	Number of Singulated Pieces/Min
1	384	535	43.06
2	386	529	43.78
3	389	541	43.14
4	383	519	44.27
Avg.	385.5	531	43.56

**Table 4.8 - Singulating Throughput for Magnet Rate of 76 magnets/min**

The singulating throughput varied from 29.24 to 44.27 pieces/min for individual test runs, over all magnet rates. The average throughput varied from 29.96 to 43.56 pieces/min. The average throughput over all test runs at all magnet rates was 35.7 pieces/min.

Comparing with Akella's results (2008), the singulation throughput varied from 15.19 to 42.37 pieces/min for individual test runs, over all magnet runs, average throughput varied from 15.59

to 35.60 pieces/min, and the average throughput over all test runs at all magnet rates was 28.41 pieces/min. There is a significant increase of 25.66% in the average throughput of all test runs at all magnet rates over Akella's machine (2008).

#### 4.2a Singulating Efficiency Results without Sensor Bed-1, Sensor Bed-2 and Electromagnets at Various Belt Speeds

This test was performed to examine the contribution of the electromagnets in controlling the silverware flow on the downward inclined plate. The only change in the experimental set up was, the sensor bed-1, sensor bed-2 and the two electromagnets were turned off throughout the tests. As a result the conveyor was kept running continuously until the silverware were completely transferred to the downward inclined plate. From section 4.1, the best results were obtained at 76 magnets/min, hence we started the tests with belt speeds at 76 magnets/min.

Case 1: Magnet rate of 76 magnets/min

Run No.	Total Number of Silverware Pieces	Number of Pieces in Twos	Number of Pieces in Threes	Number of Pieces in Groups	Number of Pieces Left Over	Number of Singulated Pieces	Singulating Efficiency %
1	400	32	12	8	4	344	86.00
2	400	28	12	4	3	353	88.25
3	400	36	18	8	0	338	84.50
4	400	34	21	0	4	341	85.25
Avg.	400	32.5	15.75	5	2.75	344	86.00

**Table 4.9 – Singulating Results without Electromagnets for Magnet Rate of 76 magnets/min**

Case 2: Magnet rate of 67 magnets/min

Run No.	Total Number of Silverware Pieces	Number of Pieces in Twos	Number of Pieces in Threes	Number of Pieces in Groups	Number of Pieces Left Over	Number of Singulated Pieces	Singulating Efficiency %
1	400	48	24	8	5	315	78.75
2	400	38	18	0	2	342	85.50
3	400	42	15	12	5	326	81.50
4	400	48	18	4	4	326	81.50
Avg.	400	44	18.75	6	4	327.25	81.81

**Table 4.10 – Singulating Results without Electromagnets for Magnet Rate of 67 magnets/min**

Case 3: Magnet rate of 59 magnets/min

Run No.	Total Number of Silverware Pieces	Number of Pieces in Twos	Number of Pieces in Threes	Number of Pieces in Groups	Number of Pieces Left Over	Number of Singulated Pieces	Singulating Efficiency %
1	400	52	18	8	7	315	78.75
2	400	48	24	12	4	312	78.00
3	400	56	18	4	3	319	79.75
4	400	48	30	12	6	304	76.00
Avg.	400	51	22.5	9	5	312.5	78.13

**Table 4.11 – Singulating Results without Electromagnets for Magnet Rate of 59 magnets/min**



Test results for magnet rate of 52 magnets/min were not collected as huge silverware cluster was accumulated at the end of the metering bin and the magnetic leather belt was incapable of pulling out individual pieces of silverware from the cluster.

The singulating efficiency varied from 88.25% to 76.00% for individual test runs, over all magnet rates. The average singulating efficiency varied from 86% to 78.13%. Comparing tables in section 4.1a and 4.2a, we observe a significant increase in the number of pieces in twos, threes, and in groups when the electromagnets are not used. The cause for such a behavior is attributed to the formation of silverware cluster of 30-40 pieces at the end of the metering bin leading to the entanglement of silverware with each other. The magnetic leather belt then pulls out pieces of two, threes, and fours from this cluster. Another observation from tables 4.9 to 4.13, is the size of the silverware cluster is dependent on the speed of the magnetic belt speed. The size of the silverware clusters inversely vary with the magnet rates, hence at a magnet rate of 76 magnets/min the silverware cluster was smaller.

#### **4.2b Throughput Results without Sensor Bed-1, Sensor Bed-2 and Electromagnets at Various Belt Speeds**

In tables 4.12 – 4.14, the run numbers indicate the corresponding runs in tables 4.9 – 4.11. This is indicated by the results in the 3<sup>rd</sup> column from the left in tables 4.12 – 4.14 being the same as the results in the seventh column from the left in tables 4.9 – 4.11 for the same magnet rates.

Case 1: Magnet rate of 76 magnets/min

Run No.	Number of Singulated Pieces	Total Time Taken (secs)	Number of Singulated Pieces/Min
1	344	555	37.19
2	353	498	42.53
3	338	512	39.61
4	341	526	38.90
Avg.	344	522.75	39.56

**Table 4.12 - Throughput Results without Electromagnets for Magnet Rate of 76 magnets/min**

Case 2: Magnet rate of 67 magnets/min

Run No.	Number of Singulated Pieces	Total Time Taken (secs)	Number of Singulated Pieces/Min
1	315	612	30.88
2	342	598	34.31
3	326	588	33.27
4	326	630	31.05
Avg.	327.25	607.00	32.38

**Table 4.13 - Throughput Results without Electromagnets for Magnet Rate of 67 magnets/min**

Case 3: Magnet rate of 59 magnets/min

Run No.	Number of Singulated Pieces	Total Time Taken (secs)	Number of Singulated Pieces/Min
1	315	635	29.76
2	312	667	28.07
3	319	654	29.27
4	304	639	28.54
Avg.	312.5	648.75	28.91

**Table 4.14 - Throughput Results without Electromagnets for Magnet Rate of 59 magnets/min**

The singulating throughput varied from 28.07 to 42.53 pieces/min for individual test runs, over all magnet rates. The average throughput varied from 28.91 to 39.56 pieces/min.

Comparing tables in section 4.1b and 4.2b, we observe a slight decrease in throughput and the total time for all the runs at various magnet rates. We expected a significant decrease in the total time taken for tests in section 4.2. But that was not the true due to formation of silverware cluster at the end of the metering bin, and the magnets from the leather belt could pick up silverware from the clusters.

Due to the significant decrease in the singulating efficiency, results from section 4.2 were not considered for the discussion section 4.4.

### **4.3 Singulation Test with Metering Bin**

Stage -01, consisting of the conveyor, sensor bed-1, sensor bed-2 and electromagnets were not considered for this test. The metering bin was loaded with 120 pieces of silverware consisting of 30 pieces each of spoons, soup spoons, forks, and knives and was continuously pulsed by the solenoid. The magnetic belt was operated at a magnet rate of 76 magnets/min. But the solenoid could not handle the load of 120 silverware pieces and failed to pulse the metering bin. Hence the load was reduced to 80 pieces of silverware. The solenoid was able to pulse the load and the silverware moved onto the plastic lined teflon cloth. However the magnets from the leather belt could not pull out pieces from the silverware cluster formed on the duck cloth as discussed in section 4.2. This silverware cluster added more load to the plastic lined teflon cloth as well. However, when tested with a load of 40 pieces of silverware the magnetic leather belt could singulate silverware pieces.

### **4.4 Discussion of Results**

Fig 4.1 shows the throughput performance for the test rig for all the test runs. It can be seen that each case, there was a little variation run-to run. Moreover, this figure shows clearly that the throughput increases with increase in magnet rate from 52 magnets/min to 76 magnets/min.

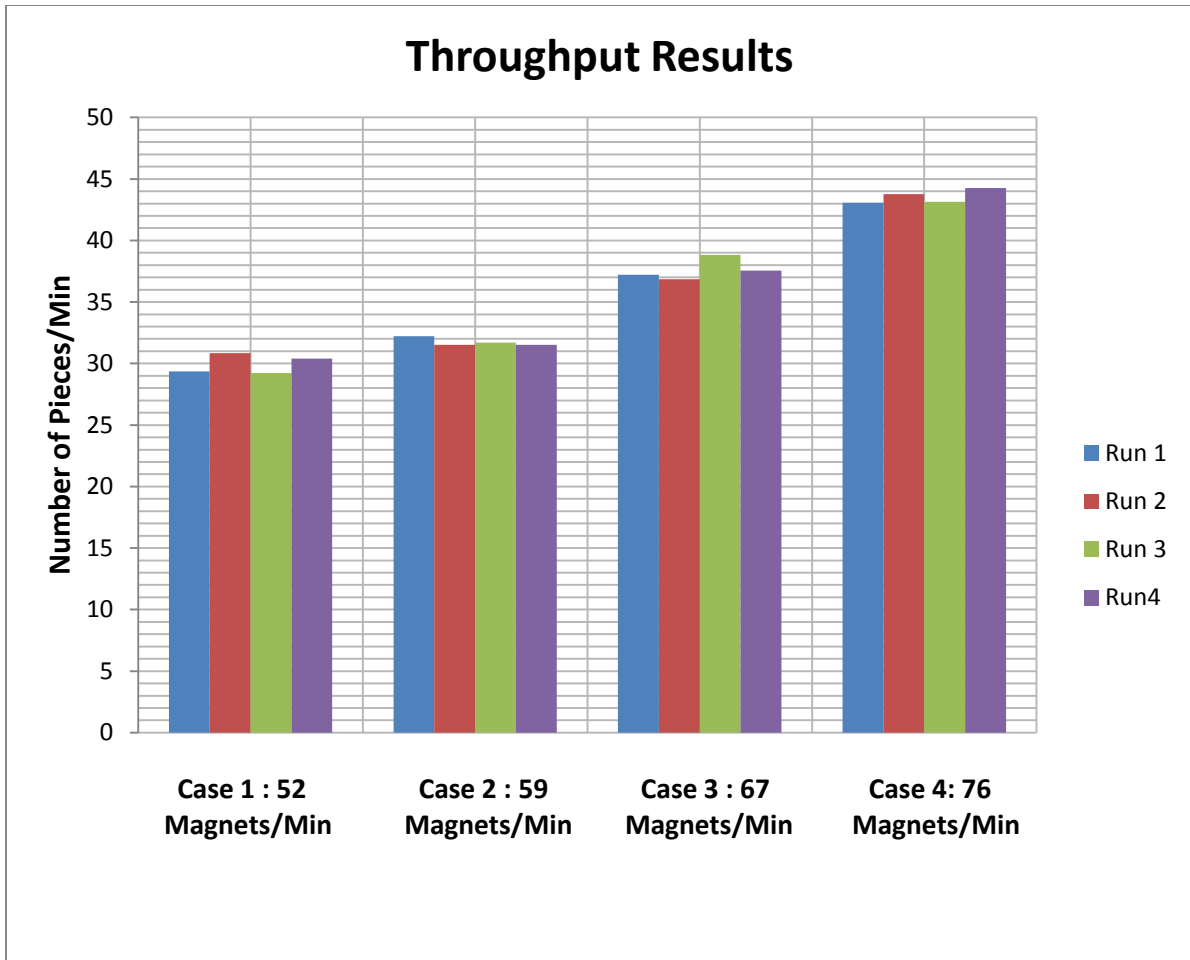
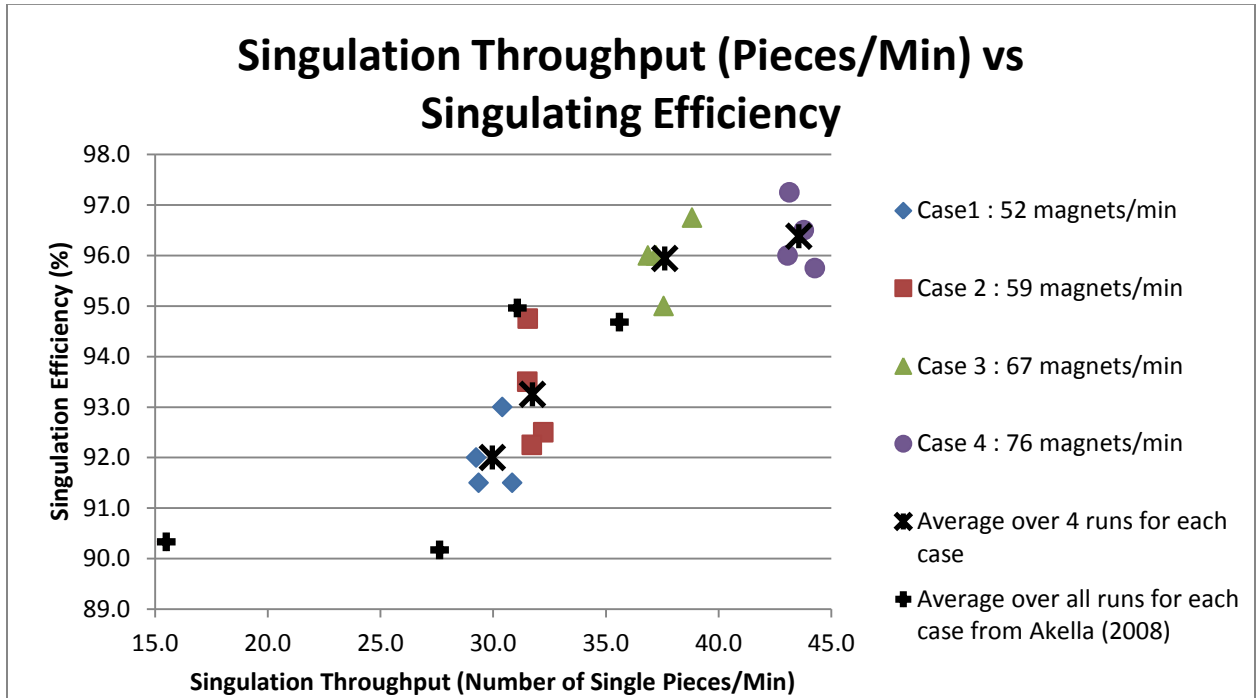


Fig. 4.1: Singulation Throughput for All Test Runs

Fig 4.2 presents a scatter plot of singulation efficiency vs. throughput. A general upward trend of singulating efficiency with singulation throughput is observed.



**Fig. 4.1: Singulating Efficiency vs Singulation Throughput (Pieces/Min) for All Test Runs**

Overall, the singulation system modified, designed, and developed in this research displayed good singulating efficiency and throughput. The best condition for operation, considering maximum singulating efficiency and maximum throughput, was at a magnet rate of 76 magnets/min, which yielded 96.38 % efficiency and 43.56 pieces/min. From Section 4.1, and 4.2 we observe that there is a 1.5% increase in the overall average singulating efficiency, and an increase of 25.66% in the overall average throughput in the current apparatus. The positive differences in the results could be attributed to:

- Improved and uniform feeding from the conveyor feed bin to the downward inclined plate.
- Reduced friction between silverware pieces and the masonite surface of the downward inclined plate by lining the plate with a thin plastic sheet. This improved silverware flow.
- Good singulation performance by the plastic lined Teflon cloth compared to the duck cloth. Plastic lined Teflon cloth had a smooth surface and offered low friction to silverware.

The singulation system could be further improved with a few design modifications that will be discussed in Chapter 5.

## CHAPTER 5

### CONCLUSIONS AND RECOMMENDATIONS

The objective of this thesis was to modify, design, construct and test an efficient mechanism to singulate silverware pieces, starting with Akella's (2008) machine. The silverware singulating machine can successfully retrieve individual silverware pieces at a reasonable throughput, and also has high singulating efficiency, as discussed in Chapter 4. The average singulating efficiency and singulating speed of Akella's machine (2008) and the present apparatus are shown in table 5.1 and 5.2 respectively:

Trials	Average Singulating Efficiency (%)	Average Throughput (Number of Single Pieces/Min)
Overall Trials <sup>1</sup>	92.90	28.41
At Best Configuration <sup>2</sup>	94.96	35.60

Overall Trials<sup>1</sup> = 24 (includes all test runs)

At Best Configuration<sup>2</sup>: At magnet rate of 67 magnets/min

**Table 5.1: Efficiency and Throughput of Akella's machine, (2008)**



Trials	Average Singulating Efficiency (%)	Average Throughput (Number of Single Pieces/Min)
Overall Trials <sup>1</sup>	94.40	35.70
At Best Configuration <sup>2</sup>	96.38	43.56

Overall Trials<sup>1</sup> = 16 (includes all test runs)

At Best Configuration<sup>2</sup>: At magnet rate of 76 magnets/min

**Table 5.2: Efficiency and Throughput of Present Setup**

Comparing Table 5.1 and 5.2, we see that there is a 1.5% increase in the average singulating efficiency for the overall trial runs and 1.42% increase in the average singulating efficiency at the best configuration in the current apparatus. However, there is a significant increase of 25.66% in the average throughput of all completed test runs over Akella's machine (2008), and an increase of 22.36% in the average throughput at the best configuration over Akella's machine (2008).

## 5.1 Contributions

Major contributions of this research are:

- Designed and developed new conveyor feed bin to improve the feeding mechanism to deliver silverware pieces to the inclined plate. As compared to Akella's vibrating bin (2008), the conveyor feed bin delivered silverware pieces more uniformly to the inclined plate and the speed of the conveyor feed bin could be easily changed by altering the software code.

- Researched, selected and implemented inductive proximity sensors to detect the presence of silverware. Due to the non-contact nature of these sensors, they do not undergo any wear as compared to the copper strip sensors used by Akella, (2008).
- Designed and installed the sensor beds at multiple locations on the inclined plate and metering bin to detect the presence of silverware.
- Reduced friction between silverware pieces and the masonite surface of the downward inclined plate by lining the plate with a thin plastic sheet. This improved silverware flow.
- Modified the metering bin, making it more reliable and efficient.
- Modified the solenoid installation, so that it could pulse the metering bin more efficiently.
- Effectively used plastic lined teflon cloth as a covering material for the moving magnet on the leather belt, which offered improved wear resistance.

## **5.2 Drawbacks**

- Neoprene, the belt material selected for conveyor feed bin promised minimal stretch when purchased. However, with repeated use the belt did stretch, for which the distance between the driven and the drive roller had to be frequently increased to maintain belt tightness.
- The cost of each inductive proximity sensor was \$16.50. We required a total of twenty one sensors for all the three sensor beds, giving a total sensor cost of \$346.50. This is expensive compared with the copper strip sensors used by Akella, (2008).

- As silverware pieces are trickled from the metering bin to the plastic lined Teflon cloth, a few silverware pieces tend to be left on the sides of the Teflon cloth and not singulated, as shown in Section 4.1.

### **5.3 Recommendations**

- Replace the Neoprene belt with another material to reduce belt stretch.
- The bottom part of the sides of the plastic coated Teflon cloth could have a hard surface so that the silverware pieces could slide down to the center and be dragged by the magnet-leather belt.
- Construct a pre-production commercial prototype from production-grade, corrosion-resistant materials and evaluate.

## REFERENCES

1. Clyde Weihi, Needham Heights; Lewis Maroti, Melrose; Peter Albertini. "Flatware Separating Apparatus", U.S. Patent – 4,954,250, September 4, 1990
2. Robert H. Chiasson, " Flatware Sorting Machine", U.S. Patent – 5,996,809, December 07, 1999.
3. Peddi Ravi, Vamshidar, "Silverware Sorting and Orienting System", M.S. Thesis, School of Mechanical and Aerospace Engineering, Stillwater, OK: Oklahoma State University, May 2005.
4. Jeyapalan, Arul Selvam Simon, "Automated Wrapping of Silverware in a Napkin", M.S. Thesis, School of Mechanical and Aerospace Engineering, Stillwater, OK: Oklahoma State University, December 2005.
5. Sabpipatana, Letrit " Silverware Singulating Machine", M.S. Thesis, School of Mechanical and Aerospace Engineering, Stillwater, OK: Oklahoma State University, May 2010.
6. Akella, Venkatesh " Silverware Singulating System", M.S. Thesis, School of Mechanical and Aerospace Engineering, Stillwater, OK: Oklahoma State University, December 2008.

## **APPENDICES**

**APPENDIX-A**

**ABSTRACTS OF PATENTS REVIEWED**

# United States Patent [19]

Weihe et al.

[11] Patent Number: **4,954,250**

[45] Date of Patent: **Sep. 4, 1990**

[54] **FLATWARE SEPARATING APPARATUS**

[75] Inventors: **Clyde Weihe, Needham Heights; Lewis Marotti, Melrose; Peter Albertini, Dover, all of Mass.**

[73] Assignee: **Food Service Innovations, Inc., Dover, Mass.**

[21] Appl. No.: **352,356**

[22] Filed: **May 16, 1989**

[51] Int. Cl.<sup>5</sup> ..... **B07C 5/12**

[52] U.S. Cl. .... **209/629; 209/632; 209/633; 209/644; 209/660; 209/673; 209/926; 209/932; 209/940**

[58] Field of Search ..... **209/44.1, 44.2, 557, 209/606, 615-618, 629, 632, 633, 644, 651-654, 656, 658, 659, 660, 667-669, 671, 673, 707, 911, 932, 940**

[56] **References Cited**

**U.S. PATENT DOCUMENTS**

909,413	1/1909	Huntley	.....	209/656
1,459,553	6/1923	Rocheleau	.....	209/673
2,340,775	2/1944	Snyder	.....	209/644
2,417,878	3/1947	Luzietti et al.	.....	209/644
3,247,858	4/1966	Kraeft	.....	209/926 X

3,545,613	12/1970	Nystuen	.....	209/926 X
3,583,564	6/1971	Peters	.....	209/616
4,635,798	1/1987	Bruck	.....	209/940 X
4,750,621	6/1988	Akesson et al.	.....	209/926 X

**FOREIGN PATENT DOCUMENTS**

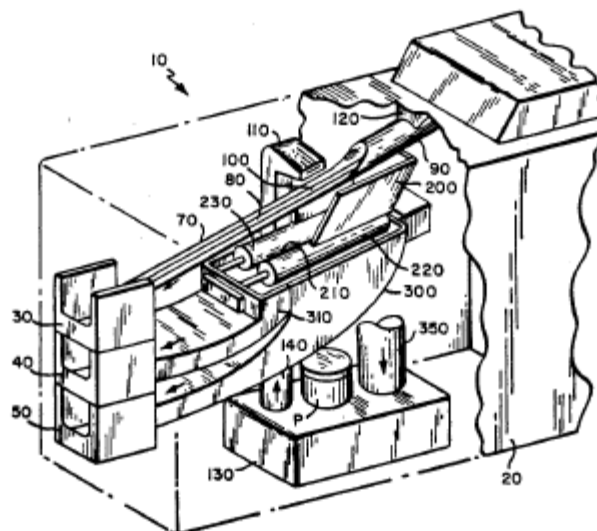
2042321	3/1972	Fed. Rep. of Germany	.....	209/926
2915993	11/1979	Fed. Rep. of Germany	.....	209/644

*Primary Examiner*—Johnny D. Cherry  
*Assistant Examiner*—Edward M. Wacyra  
*Attorney, Agent, or Firm*—M. Lawrence Oliverio

[57] **ABSTRACT**

A flatware separating apparatus comprising a track having a top surface for receiving and delivering different items of flatware along a selected path; a mechanism for contacting selected items of the flatware at a selected point along the path of the track and pushing the selected items off the surface of the track and allowing other selected items of the flatware to remain on the surface; and a mechanism for further separating the selected items of flatware pushed off the surface of the track.

**39 Claims, 5 Drawing Sheets**





US005996809A

**United States Patent** [19]  
**Chiasson**

[11] **Patent Number:** **5,996,809**  
[45] **Date of Patent:** **Dec. 7, 1999**

[54] **FLATWARE SORTING MACHINE**  
[76] **Inventor:** **Robert H. Chiasson**, c/o East Coast Industries, Inc. 2532 Main St., Concord, Mass. 01742

4,220,240 9/1980 Narberg et al. .... 198,681 X  
4,744,469 5/1988 Swallert ..... 209,926 X  
5,379,880 1/1995 Stone et al. .... 198,679 X

**FOREIGN PATENT DOCUMENTS**

2170737 8/1986 United Kingdom ..... 209,926

[21] **Appl. No.:** **08/852,088**

[22] **Filed:** **May 7, 1997**

[51] **Int. Cl.<sup>6</sup>** ..... **B07C 5/344; B65G 17/32**

[52] **U.S. Cl.** ..... **209/636; 209/904; 209/919;**  
209/926; 198/443; 198/679; 198/681; 198/803.6

[58] **Field of Search** ..... 209/636, 904,  
209/907, 919, 926; 198/678.1, 679, 681,  
690.1, 803.6, 443

*Primary Examiner*—Tuan N. Nguyen  
*Attorney, Agent, or Firm*—Iandiorio & Teska

[57] **ABSTRACT**

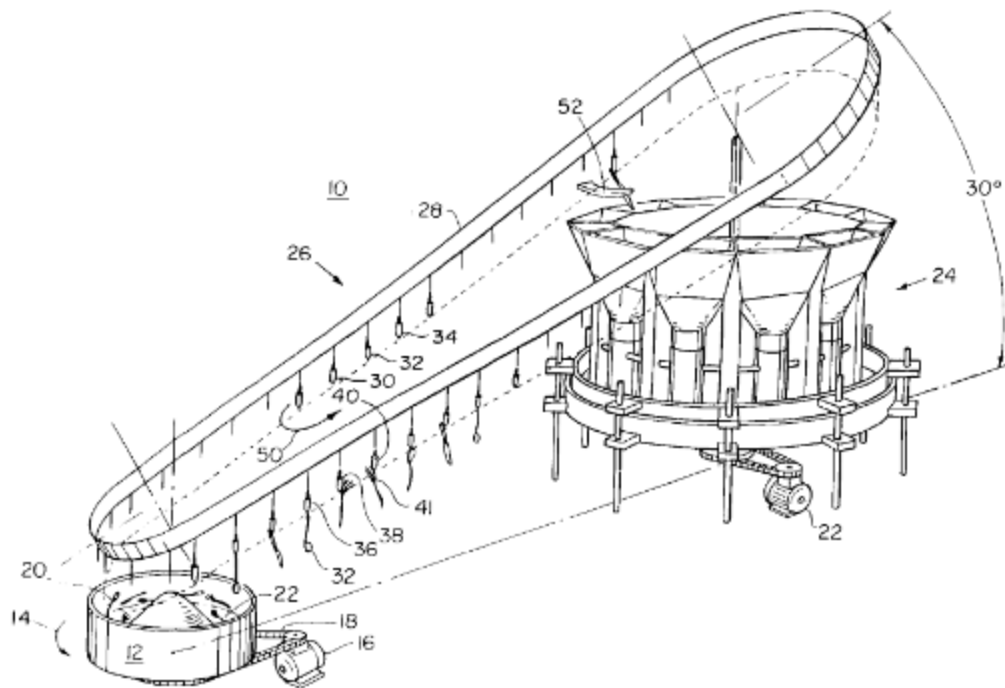
A flatware sorting machine including a feed bin for holding unsorted flatware, a sorting system for sorting the flatware, and a flatware pick-up and transport system for retrieving the flatware from the feed bin and transporting them to the sorting system.

[56] **References Cited**

**U.S. PATENT DOCUMENTS**

3,948,386 4/1976 Nalbach ..... 198/443 X

**16 Claims, 12 Drawing Sheets**





## **APPENDIX-B**

### **WEBSITES REFERENCED**

**[1] "Inductive Proximity Sensors". Altech Corp. Retrieved 27 Oct. 2011**

**[2] "Proximity Sensor Technology". Automation Direct. Retrieved 27 Oct. 2011**

## **APPENDIX-C**

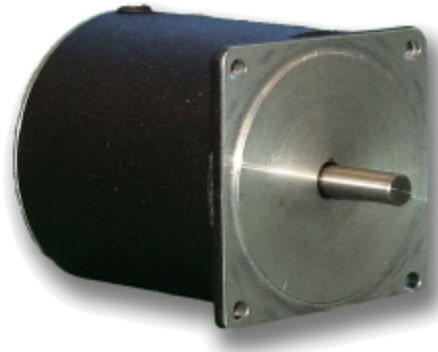
### **DATASHEET FOR CONVEYOR FEED BIN STEPPER MOTOR**

## 34W Series - Standard Torque Stepper Motors



### FEATURES

- NEMA Size 34 Round Stepper Motor
- Best Selection for High Speed Applications
- 1.8° Step Angle
- Torque - Up to 700 oz-in
- Can be Customized for
  - Winding Current
  - Shaft Options
  - Cables and Connectors
- CE Certified and RoHS Compliant



### DESCRIPTION

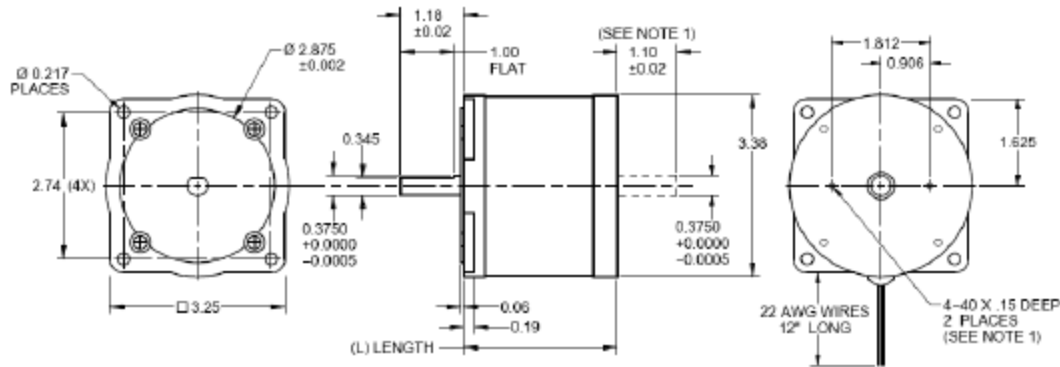
The 34W Series Stepper Motors offer a very high value for a standard (round-bodied) style stepper motor. They have lower rotor inertia than square high torque motors which allow them to accelerate faster and offer higher torque at speeds greater than 25 revolutions per second. These motors are an excellent choice to replace many of the round stepper motors that were popular for many years. The motor comes in a standard 8-lead configuration with a broad line of motor windings and stack lengths available off-the-shelf. Anaheim Automation can also customize the winding to perfectly match your voltage, current, and maximum operating speed. Special shaft modifications, cables and connectors are also available upon request.

### SPECIFICATIONS

Model #	NEMA Size	Bipolar Torque (oz-in)	Series Current (A)	Unipolar Current (A)	Parallel Current (A)	Unipolar Inductance (mH)	Rotor Inertia (oz-in-sec <sup>2</sup> )	Shaft Diameter (in)	# of Lead Wires	Weight (lbs)	L Length (in)
34W109S-LW8	34	345	3.5	4.5	6.4	1.4	0.008	0.375	8	3.3	2.44
34W207S-LW8	34	467	2.5	3.5	5.0	3.3	0.017	0.375	8	5.7	3.70
34W214S-LW8	34	467	4.9	7.0	9.9	0.7	0.017	0.375	8	5.7	3.70
34W307S-LW8	34	708	2.5	3.5	4.9	5.9	0.027	0.375	8	8.4	5.27
34W311S-LW8	34	708	4.3	6.5	9.2	2.4	0.027	0.375	8	8.4	5.27
34W314S-LW8	34	708	4.9	7.0	9.9	1.2	0.027	0.375	8	8.4	5.27

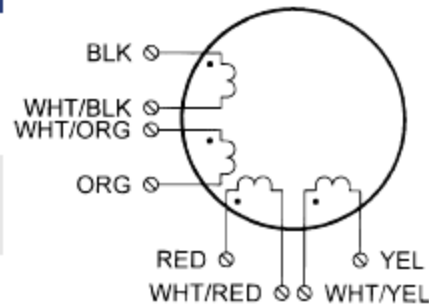
Notes: The 7th character "S" denotes a single shaft, use "D" for double shaft. Custom leadwires, cables, connectors, and windings are available upon request.

L010215



(All units are inches)

Connection	Lead Wire Connection	Lead Wire Color
4-Lead Bipolar Series MBC, MLP or MJA Series	Phase 1 (A)	Black
	Phase 3 (X)	Orange
	Phase 2 (E)	Red
	Phase 4 (B)	Yellow
	Connect Wires with Wire Nut Connect Wires with Wire Nut	White/Black & White/Orange White/Red & White/Yellow
4-Lead Bipolar Parallel MBC, MLP or MJA Parallel	Phase 1 (A)	Black & White/Orange
	Phase 3 (X)	Orange & White/Black
	Phase 2 (E)	Red & White/Yellow
	Phase 4 (B)	Yellow & White/Red
6-Lead Unipolar BLD, TM Series	Phase 1	Black
	Phase 3	Orange
	Phase 2	Red
	Phase 4	Yellow
	Common Phase 1 & 3 Common Phase 2 & 4	White/Black & White/Orange White/Red & White/Yellow



Step Angle Accuracy:	+/- 5% (full step, no load)	Insulation Resistance:	100M Ohm, Min. 500VDC
Resistance Accuracy:	+/- 10%	Dielectric Strength:	500VAC
Inductance Accuracy:	+/- 20%	Radial Play:	0.02" at 1.0 lbs
Temperature Rise:	80°C Max (2 phase on)	End Play:	0.08" at 1.0 lbs
Ambient Temperature:	-20°C to +50°C	Max Radial Force:	16.9 lbs (0.79" from flange)
Insulation Type:	Class B	Max Axial Force:	3.37 lbs

## **APPENDIX-D**

### **DATASHEET FOR STEPPER MOTOR DRIVER**

## MBC12101 - Microstep Driver

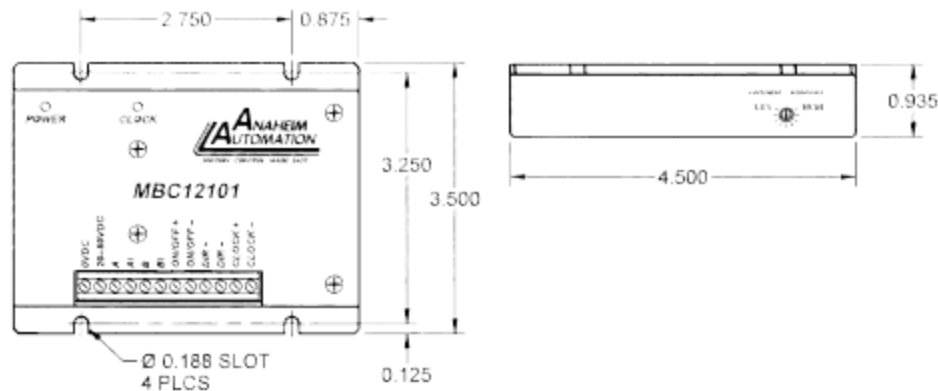


### FEATURES

- Compact Stepper Motor Driver
- 1.5 - 10.0 Amp Current Range
- 2000 Steps per Revolution
- Optically Isolated Inputs
- Short Circuit Protection
- 20 - 80VDC Bus Voltage
- Automatic Current Reduction
- Sinking and Sourcing Inputs
- Power and Clock LEDs



### DIMENSIONS



### DESCRIPTION

If you're looking for big time stepper performance from a small driver, the MBC12101 is your answer. This powerful microstepping driver provides excellent torque in a compact and low profile enclosure. The MBC12101 is also very easy to use. It features rugged terminal blocks, a rotary pot for current settings, and a visible silkscreen for easy installation.

Versatile as well as powerful, the MBC12101 has a wide amperage range. It is designed to handle small stepper motors rated as low as 1.5 Amps/phase, mid-sized steppers such as NEMA 23's and 34's, as well as larger motors with current ratings up to 10.0 Amps. It operates from a DC voltage of 20-80 Volts, making it a great fit for almost any stepper application.

The MBC12101 features optically isolated inputs that are 3.5 - 8.6VDC compatible. The clock input can be set to receive either sinking or sourcing clock signals at frequencies up to 100KHz. The driver also features direction control, motor on/off capabilities, and a built in short circuit and miswire shutdown protection.

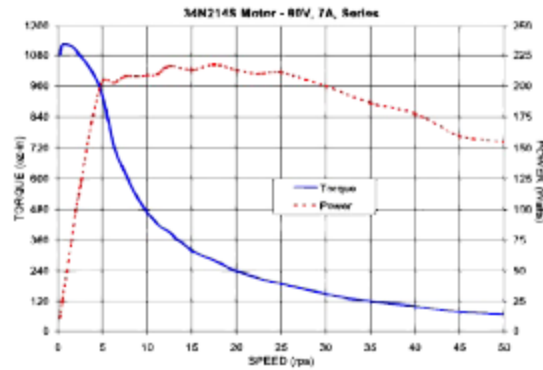
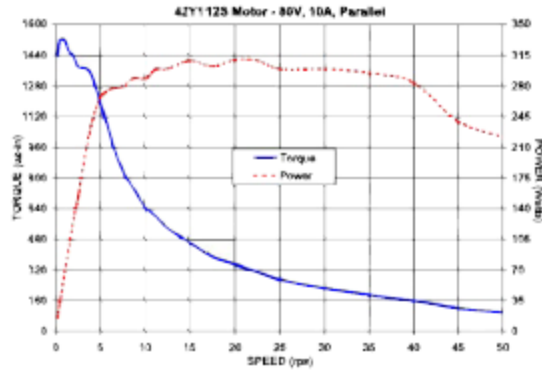
The MBC12101 is a bipolar type driver designed for use with 4, 6, or 8 lead stepper motors, making it compatible for series and parallel installations. The driver has a 2000 steps per revolution or 0.18° per step resolution, with respect to a 1.8° stepper motor. It also has a motor current reduction feature that will help keep stepper motors cool at standstill, and LEDs that indicate power and pulses being received.

#### Ideal Applications:

Automated machinery or processes that involve food, cosmetic, or medical packaging, labeling, or tamper-evident requirements, cut-to-length applications, electronic assembly, robotics, factory automation, special filming and projection effects, medical diagnostics, inspection and security devices, conveyor and material handling systems, metal fabrication (CNC machinery), pump flow control, XY and rotary tables, equipment upgrades or wherever precise positioning or speed control is required.



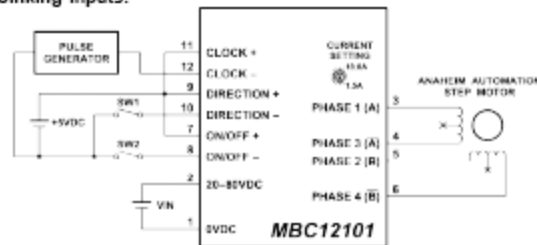
## Torque Speed Curves



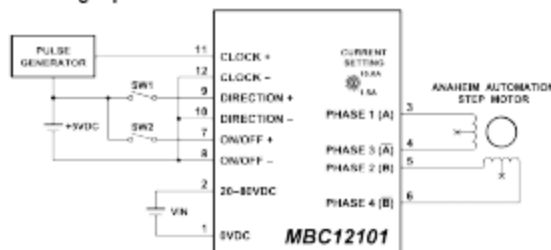
## Specifications

<b>Power Requirements:</b>	20 - 80 VDC
<b>Output Current Range:</b>	1.5 - 10.0 Amps (Peak)
<b>Microstepping Resolution:</b>	2000 Steps/Revolution (Div-by-10)
<b>Input Signal Voltage:</b>	3.5 - 8.6 VDC
<b>Input Clock Frequency:</b>	0 - 100 KHz
<b>Minimum Input Current:</b> (Isolated Inputs)	1.0 mA
<b>Storage Temperature:</b>	0° - 50° C
<b>Absolute Maximum Driver Temperature:</b>	70° C
<b>Driver Type:</b>	Bipolar, Compatible with 4, 6, and 8 Lead Motors, Series or Parallel connection.

### Sinking Inputs:



### Sourcing Inputs:



## Additional Ordering Information

Model #	Description	Input Voltage	Power (Watt)
PSA80V4A-1	80 VDC Power Supply, Up to 4.0 Amp Capability	110 or 220 VAC	320
PSA40V4A	40 VDC Power Supply, Up to 4.0 Amp Capability	110 or 220 VAC	160
PCL601	Single Axis Simple Programmable Controller, RS232/485 Compatible	24 VDC	-
PCL601USB	Single Axis Simple Programmable Controller, USB Compatible	24 VDC	-
MBC10101-75	Enhanced Performance 10A Microstep Driver	8 - 55VDC	-
MBC10S11	MBC10101 with a simple indexer, USB compatible	20 - 80VDC	-
MBC10P31	MBC10101 with a pulse generator, USB compatible	20 - 80VDC	-

910 East Orangefair Ln. Anaheim, CA 92801 Tel. (714) 992-6990 Fax. (714) 992-0471 [www.anaheimautomation.com](http://www.anaheimautomation.com)

ADDITIONAL INFORMATION



## **APPENDIX-E**

### **DATASHEET FOR INDUCTIVE PROXIMITY SENSOR**

# PB Series Inductive Proximity Sensors

## Nickel-plated Brass - DC



**PBT-AN-1H**   **PBT-AN-2H**

- Low cost/high performance
- Twelve models available
- IP67 rated
- LED status indicators
- M12 quick-disconnect; order cable separately
- Lifetime warranty

Basic Series Inductive Prox Selection Chart								
Part Number	Price	Sensing Range	Housing	Output State	Logic	Connection	Wiring	Dimensions
<b>M12 Models</b>								
<a href="#">PBM-AN-1H</a>	<-->	2 mm (0.079 in)	Shielded	N.O.	NPN	M12 (12 mm) connector	Diagram 1	Figure 1
<a href="#">PBM-AP-1H</a>	<-->				PNP	M12 (12 mm) connector	Diagram 2	
<a href="#">PBM-AN-2H</a>	<-->	4 mm (0.157 in)	Unshielded		NPN	M12 (12 mm) connector	Diagram 1	
<a href="#">PBM-AP-2H</a>	<-->				PNP	M12 (12 mm) connector	Diagram 2	
<b>M18 Models</b>								
<a href="#">PBK-AN-1H</a>	<-->	5 mm (0.197 in)	Shielded	N.O.	NPN	M12 (12 mm) connector	Diagram 1	Figure 2
<a href="#">PBK-AP-1H</a>	<-->				PNP	M12 (12 mm) connector	Diagram 2	
<a href="#">PBK-AN-2H</a>	<-->	8 mm (0.315 in)	Unshielded		NPN	M12 (12 mm) connector	Diagram 1	
<a href="#">PBK-AP-2H</a>	<-->				PNP	M12 (12 mm) connector	Diagram 2	
<b>M30 Models</b>								
<a href="#">PBT-AN-1H</a>	<-->	10 mm (0.394 in)	Shielded	N.O.	NPN	M12 (12 mm) connector	Diagram 1	Figure 3
<a href="#">PBT-AP-1H</a>	<-->				PNP	M12 (12 mm) connector	Diagram 2	
<a href="#">PBT-AN-2H</a>	<-->	15 mm (0.590 in)	Unshielded		NPN	M12 (12 mm) connector	Diagram 1	
<a href="#">PBT-AP-2H</a>	<-->				PNP	M12 (12 mm) connector	Diagram 2	

## Wiring diagrams

**Diagram 1**

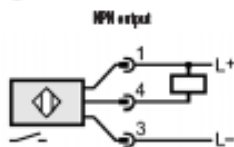
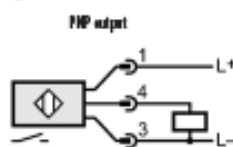


**Diagram 2**



**M12 Connector**



**Cable Assembly Wiring Colors:**  
**Pin 1 - Brown**  
**Pin 3 - Blue**  
**Pin 4 - Black**

# PB Series Inductive Proximity Sensors

Specifications	M12 Models		M18 Models		M30 Models	
	Shielded	Unshielded	Shielded	Unshielded	Shielded	Unshielded
Type	Shielded	Unshielded	Shielded	Unshielded	Shielded	Unshielded
Operating Distance	2 mm (0.079 in)	4 mm (0.157 in)	5 mm (0.197 in)	8 mm (0.315 in)	10 mm (0.394 in)	15 mm (0.590 in)
Material Correction Factors	See Material Influence table #2 later in this section.					
Switch-point Drift	-10 to 10% Sr					
Hysteresis	1 to 20% Sr					
Operating Voltage	15 to 30 VDC					
Current Consumption	<15 mA					
Load Current	100 mA					
Short-circuit Protection	Yes, pulsed					
Reverse Polarity Protection	Yes					
Overload Protection	Yes					
Voltage Drop	<2.5 V					
Output Type	NPN or PNP, N.O. only					
Leakage Current	<0.1 mA					
Switching Frequency	800Hz		400Hz		300Hz	
Temperature Range (Operating)	-25° to 70°C (-13° to 158°F)					
Protection Degree (DIN 40050)	IEC IP67					
Shock Resistance	IEC 60947-5-2 part 7, 4, 2					
Vibration Resistance	IEC 60947-5-2 part 7, 4, 1					
Agency Approvals	cULus file E328811, CE, RoHS					
LED Indicators / Switching Status	Yellow (output energized)					
Housing Material	Housing: brass, nickel-plated; Lock nuts: brass					
Sensing Face Material	Polybutylene Terephthalate (PBT)					
Tightening Torque	7.0 Nm (5.16 lb/ft)		35.0 Nm (25.8 lb/ft)		50.0 Nm (36.8 lb/ft)	
Weight	1.70 g (0.06 oz)		2.83 g (0.10 oz)		8.50 g (0.30 oz)	
Connectors	M12 connector 2 lock nuts included					

## Dimensions

mm [inches]

Figure 1

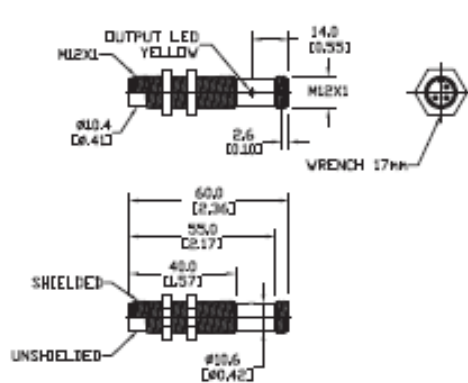


Figure 2

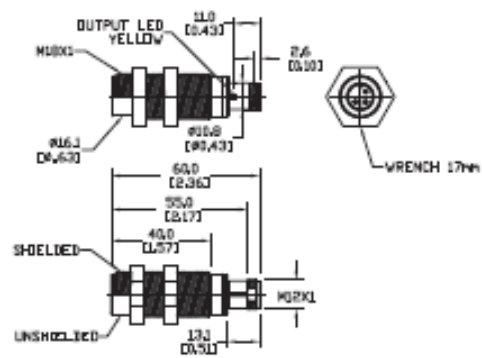
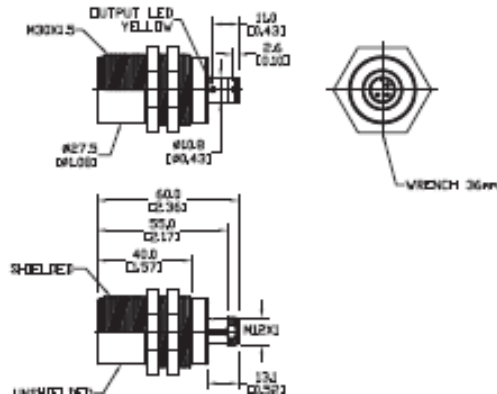


Figure 3



# Sensors Accessories: Cables

## Cables with quick-disconnect plugs

- Industry standard axial and right-angle M8/M12 screw-lock connectors with open leads. The cables listed can be used with patch cables
- 2m, 5m, 7m and 10m cable lengths

- PVC (polyvinyl chloride) jacket for typical industrial applications
- PUR (polyurethane) jacket for oily and direct sunlight applications
- IP67 rated



M8 Quick-Disconnect Cables (Pico, Nano)							
Part Number	Price	Length	Poles	Connector	LED	Jacket	Dimensions
<i>M8 Quick-Disconnects</i>							
<a href="#">CD08-0A-020-A1</a>	<->	2m (6.5ft.)	3	Axial	No	PVC	Figure 1
<a href="#">CD08-0A-020-C1</a>	<->	2m (6.5ft.)	3	Right-angle	No	PVC	Figure 2
<a href="#">CD08-0A-050-A1</a>	<->	5m (16.4ft.)	3	Axial	No	PVC	Figure 4
<a href="#">CD08-0C-050-A1</a>	<->	5m (16.4ft.)	3	Axial	No	PUR	Figure 3
<a href="#">CD08-0A-050-C1</a>	<->	5m (16.4ft.)	3	Right-angle	No	PVC	Figure 5
<a href="#">CD08-0C-050-C1</a>	<->	5m (16.4ft.)	3	Right-angle	No	PUR	Figure 5
<a href="#">CD08-0A-070-A1</a>	<->	7m (23ft.)	3	Axial	No	PVC	Figure 1
<a href="#">CD08-0A-070-C1</a>	<->	7m (23ft.)	3	Right-angle	No	PVC	Figure 2

M12 Quick-Disconnect Cables (Euro, Micro DC-Single Key)							
Part Number	Price	Length	Poles	Connector	LED	Jacket	Dimensions
<i>M12 Quick-Disconnects</i>							
<a href="#">CD12L-0B-020-A0</a>	<->	2m (6.5ft.)	4	Axial	No	PVC	Figure 6
<a href="#">CD12L-0B-020-C0</a>	<->	2m (6.5ft.)	4	Right-angle	No	PVC	Figure 7
<a href="#">CD12M-0B-050-A1*</a>	<->	5m (16.4ft.)	3	Axial	No	PVC	Figure 8
<a href="#">CD12M-0D-050-A1*</a>	<->	5m (16.4ft.)	3	Axial	No	PUR	Figure 9
<a href="#">CD12M-0B-050-C1*</a>	<->	5m (16.4ft.)	3	Right-angle	No	PVC	Figure 10
<a href="#">CD12M-0D-050-C1*</a>	<->	5m (16.4ft.)	3	Right-angle	No	PUR	Figure 11
<a href="#">CD12M-0B-070-A1</a>	<->	7m (23ft.)	4	Axial	No	PVC	Figure 6
<a href="#">CD12M-0B-070-C1</a>	<->	7m (23ft.)	4	Right-angle	No	PVC	Figure 7

\* Note: Do not use with: DM, FA, OX, SS, SSF, SU, TU, VM, VK, MV, MS or MSF series sensors. These sensors require 4-pole cables.

CD12M-0B-050-C1 and -A1 shown

## Cables with LED and quick-disconnect plugs

- Industry standard M12 right angle female plug with open leads
- These cables can be used with patch cables
- 2m, 5m and 10m cable lengths

- PUR (polyurethane) jacket for oily and direct sunlight applications
- IP67 /IP68 / IP69K, II rated
- LED indication for 10 -36 VDC PNP sensors only



M12 Quick-Disconnect Cables with LED Indicator (Euro, Micro DC-Single Key)							
Part Number	Price	Length	Poles	Connector	LED	Jacket	Dimensions
<i>M12 Quick-Disconnects</i>							
<a href="#">EVC178*</a>	<->	2m (6.5ft.)	4	Right-angle	Yes	PUR	Figure 12
<a href="#">EVC179*</a>	<->	5m (16.4ft.)	4	Right-angle	Yes	PUR	Figure 12
<a href="#">EVC180*</a>	<->	10m (32.8ft.)	4	Right-angle	Yes	PUR	Figure 12

\*Note: LED for 10 to 36 VDC PNP only.  
Do not use when white wire (Pin 2) is used for selection of a sensor function.

### LED Models' Wiring



# Sensors Accessories: Cables

Cable Specifications					
Specification	M8		M12		M12 with LED
Length	2m (6.5ft) / 7m (23ft)	5m (16.4ft)	2m (6.5ft) / 7m (23ft)	5m (16.4ft)	2m (6.5 ft) / 5m (16.4ft) / 10m (32.8ft)
Nominal Voltage	50VAC/75VDC	60VAC/DC	300VAC	250VAC/DC	10 to 36VDC
Max Current	4A		4A		4A
LED Current Loading	N/A	N/A	N/A	N/A	10V input Brown wire LED: 1.7mA White and/or Black LED: 0.9mA 36V input Brown wire LED: 7.3mA White and/or Black LED: 4.7mA
Protection Degree	IP67	IP65 / IP68 / IP69K	IP67	PVC: IP68 PUR: IP68 / IP69K	IP67 / IP68 / IP69K
Material Nut	brass; nickel plated		brass; nickel plated		brass; nickel plated
Jacket Material	PVC	PVC:CD08-0A-xxx PUR:CD08-0C-xxx	PVC	PVC:CD12M-0B-xxx PUR:CD12M-0D-xxx	PUR
Housing Material	PUR		PUR		PUR
Contacts Material	Copper-Tin Alloy (CuSn) -gold plated		Copper-Tin Alloy (CuSn) -gold plated		Gold plated brass
Tightening Torque	0.5 Nm	≤ 0.4 Nm	0.5 Nm	≤ 0.4 Nm	0.6 to 1.5 Nm
Conductors Cross Section (AWG)	0.25mm <sup>2</sup> (24 AWG)	0.25mm <sup>2</sup> (24 AWG)	0.25mm <sup>2</sup> (24 AWG)	0.34mm <sup>2</sup> (22 AWG)	4 x 0.34mm <sup>2</sup> (4 x 22 AWG)
Ø Outer Cable	5mm	PVC: 4 mm PUR: 4 mm	5mm	PVC: 4.2 mm PUR: 4.3 mm	5mm
Temperature Range	-25° to +80°C (-13° to 176°F)	-25° to 90°C (-13° to 194°F)	-25° to +80°C (-13° to 176°F)	PVC: -30° to 70°C (-22° to 158°F) PUR: -50° to 90°C (-58° to 194°F)	-25° to +90°C (-13° to 194°F)
Environmental	N/A	Halogen free, Silicone free	N/A	Halogen free, Silicone free	Halogen free, Silicone free
Function Display Power LED	N/A	N/A	N/A	N/A	Green
Switching Status LED	N/A	N/A	N/A	N/A	2 x Yellow
Drag Chain (Roller Cable Tray) Suitability	Bending Radius	min. 10 x cable diameter			
	Bending Cycles	N/A	N/A	N/A	>5 million
	Travel Speed	N/A	N/A	N/A	Max. 3.3 m/s for a horizontal travel length of 5 meters and max. acceleration of 5 m/s <sup>2</sup>
	Torsional Strain	N/A	N/A	N/A	±180°/m
Agency Approvals	RoHS				UL File E191684, RoHS

UL Reference	
Part Number	Mini-Series Female Cord Connectors Series M12, UL Catalog Number
<a href="#">EVC178</a>	ADOAH043MSS002H04
<a href="#">EVC179</a>	ADOAH043MSS005H04
<a href="#">EVC180</a>	ADOAH043MSS001CH04
Note: Shown in UL file under Mini-series Female Cord Connectors using catalog number	

# Sensors Accessories: Cables

Dimensions (in/mm)

Figure 1

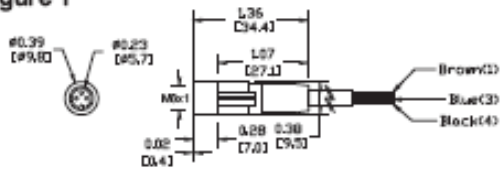


Figure 2

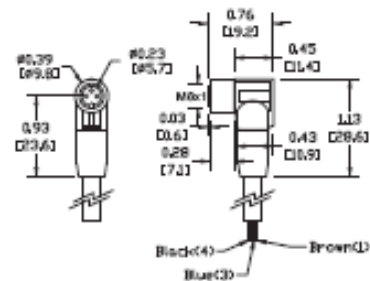


Figure 3

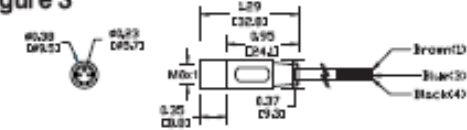


Figure 4

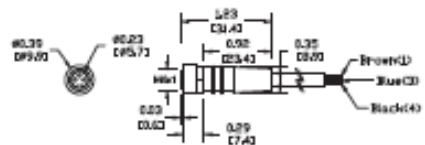


Figure 5

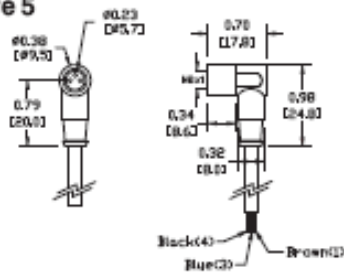


Figure 6

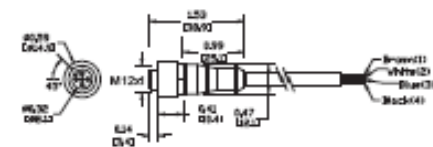


Figure 7

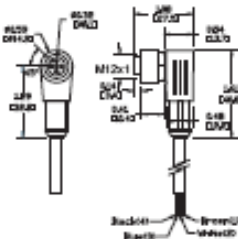


Figure 8

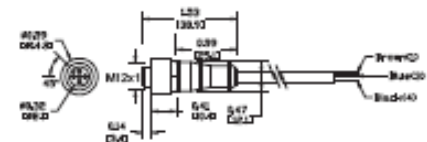


Figure 9

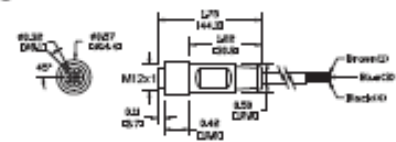


Figure 10

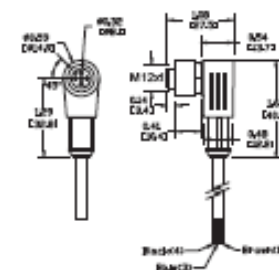


Figure 11

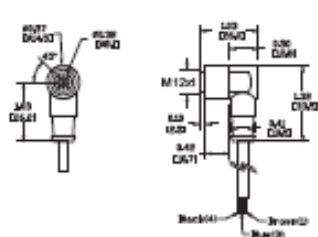
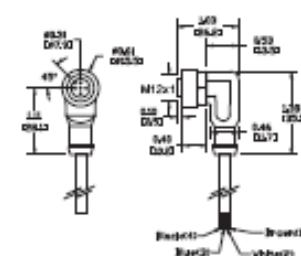


Figure 12





# Sensors Accessories: Cables

## Patch cables with quick-disconnect plugs on each end

Available patch cables include:

- Industry standard M8 and M12 screw-lock connectors
- One male and one female connector

- Axial and right-angle connector models
- 1m and 3m cable lengths
- PVC (polyvinyl chloride) jacket for typical industrial applications
- IP67 rated



M8 Patch Cables w/Quick-Disconnect on Each End (Pico, Nano)						
Part Number	Price	Length	Poles	Connectors	Jacket	Dimensions
<b>M8 Quick-Disconnect Patch Cables</b>						
<a href="#">CDP08-0A-010-AA</a>	<-->	1m (3.28ft)	3	2 Axial, One male and one female connector	PVC	Figure 1
<a href="#">CDP08-0A-010-BB</a>	<-->	1m (3.28ft)	3	2 Right-angle, One male and one female connector	PVC	Figure 3
<a href="#">CDP08-0A-030-AA</a>	<-->	3m (9.84ft)	3	2 Axial, One male and one female connector	PVC	Figure 2
<a href="#">CDP08-0A-030-BB</a>	<-->	3m (9.84ft)	3	2 Right-angle, One male and one female connector	PVC	Figure 3

M12 Patch Cables w/Quick-Disconnect on Each End (Euro, Micro DC-Single Key)						
Part Number	Price	Length	Poles	Connectors	Jacket	Dimensions
<b>M12 Quick-disconnect Patch Cables</b>						
<a href="#">CDP12-0B-010-AA</a>	<-->	1m (3.28ft)	4	2 Axial, One male and one female connector	PVC	Figure 4
<a href="#">CDP12-0B-010-BB</a>	<-->	1m (3.28ft)	4	2 Right-angle, One male and one female connector	PVC	Figure 5
<a href="#">CDP12-0B-030-AA</a>	<-->	3m (9.84ft)	4	2 Axial, One male and one female connector	PVC	Figure 4
<a href="#">CDP12-0B-030-BB</a>	<-->	3m (9.84ft)	4	2 Right-angle, One male and one female connector	PVC	Figure 5

## Patch Cables with LED

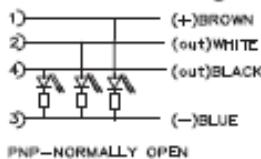
Available patch cables with LED include:

- Right-angle M12 female plug with LED indication on one end and axial male plug on the other end
- 0.3m, 0.6m, 1m, 2m, 5m, and 10m cable lengths

- PUR (polyurethane) jacket for oily and direct sunlight applications
- IP67 /IP68 / IP69K, II rated
- LED indication for 10 -36 VDC PNP sensors only



### LED Models' Wiring



M12 Patch Cables with LED Indicator (Euro, Micro DC-Single Key)								
Part Number	Price	Length	Poles	Connectors	LED	Jacket	Dimensions	
<b>M12 Patch Cables</b>								
<a href="#">EVC322<sup>+</sup></a>	<-->	0.3m (0.98ft)	4	Right-angle female, axial male	Yes	PUR	Figure 6	
<a href="#">EVC323<sup>+</sup></a>	<-->	0.6m (1.97ft)	4	Right-angle female, axial male	Yes	PUR	Figure 6	
<a href="#">EVC324<sup>+</sup></a>	<-->	1m (3.28ft)	4	Right-angle female, axial male	Yes	PUR	Figure 6	
<a href="#">EVC325<sup>+</sup></a>	<-->	2m (6.5ft)	4	Right-angle female, axial male	Yes	PUR	Figure 6	
<a href="#">EVC326<sup>+</sup></a>	<-->	5m (16.4ft)	4	Right-angle female, axial male	Yes	PUR	Figure 6	
<a href="#">EVC327<sup>+</sup></a>	<-->	10m (32.8ft)	4	Right-angle female, axial male	Yes	PUR	Figure 6	

Note: LED for 10 to 36 VDC PNP only.  
 Do not use when white wire (Pin 2) is used for selection of a sensor function.

# Sensors Accessories: Cables

Cable Specifications			
Specification	M8	M12	M12 with LED
Length	1m (3.28ft.) / 3m (9.84ft.)		0.3m (0.98ft) / 0.6m (1.97ft) / 1m (3.28ft) 2m (6.5ft) / 5m (16.4ft) / 10m (32.8ft)
Nominal Voltage	60 VAC/DC	250 VAC/DC	10 to 36VDC
Max Current	4A		4A
LED Current Consumption	N/A		10V input Brown wrg. LED: 1.7mA White and/or Black LED: 0.9mA 36V input Brown wrg. LED: 7.3mA White and/or Black LED: 4.7mA
Protection Degree	IEC IP67		IEC IP67/IP68/IP69K
Material Nut	Brass: nickel plated		Brass: nickel plated
Jacket Material	PVC		PUR
Housing Material	PUR		Connector: Orange PUR, Socket: Black PUR
Contacts Material	Copper-tin(CuSn)-Brass		Brass: gold plated
Conductors Cross Section (AWG)	0.34mm <sup>2</sup>		0.34mm <sup>2</sup> (22 AWG)
Tightening Torque	0.5 Nm		Plug: 0.6 to 1.5 Nm (take into account the maximum value of the counterpart) Socket: 0.6 to 1.5 Nm
Ø Outer Cable	5mm		5mm
Temperature Range	-25° to +70°C (-13° to 158°F)		-25° to +90°C (-13° to 194°F)
Function Display LED	N/A		Green
Switching Status LED	N/A		2 x Yellow
Drag Chain (Roller Cable Tray) Suitability	Bending Radius	min. 10 x cable diameter	
	Bending Cycles	>5 million	
	Travel Speed	N/A	Max. 3.3 m/s for a horizontal travel length of 5 m and max. acceleration of 5 m/s <sup>2</sup>
	Torsional Strain	N/A	±180°/m
Agency Approvals	RoHS		UL File E191684, RoHS

UL Reference	
Part Number	Cable Assemblies Series M12, UL Catalog Number
<a href="#">EVC322</a>	VDDAH043MSS00.3H04STGH040MSS
<a href="#">EVC323</a>	VDDAH043MSS00.6H04STGH040MSS
<a href="#">EVC324</a>	VDDAH043MSS001H04STGH040MSS
<a href="#">EVC325</a>	VDDAH043MSS002H04STGH040MSS
<a href="#">EVC326</a>	VDDAH043MSS005H04STGH040MSS
<a href="#">EVC327</a>	VDDAH043MSS010H04STGH040MSS
Note: Shown in UL file under Cable Assemblies using catalog number	



# Sensors Accessories: Cables

Dimensions (in/mm)

Figure 1

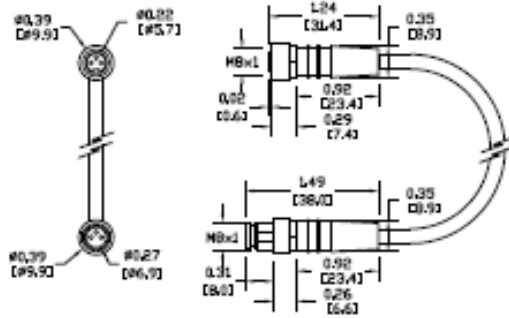


Figure 2

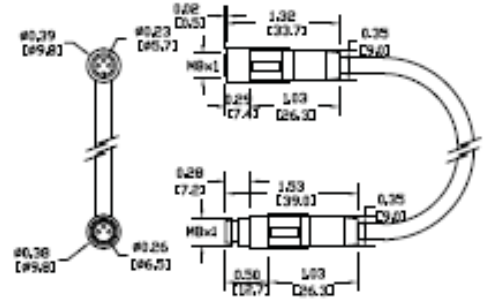


Figure 3

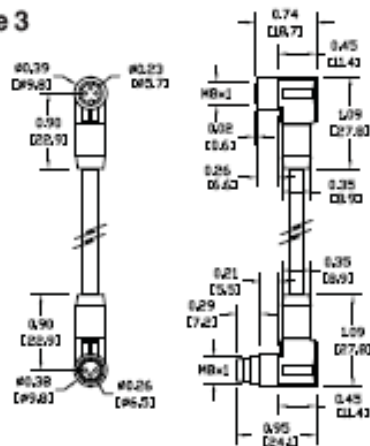


Figure 4

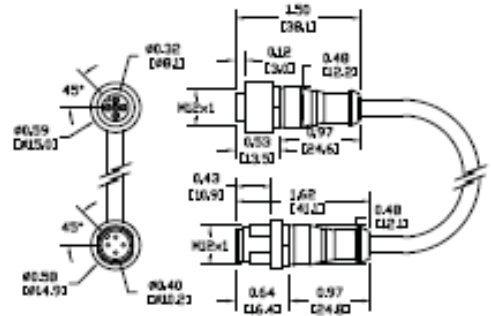


Figure 5

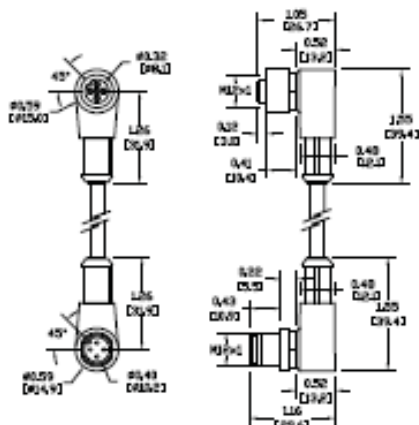
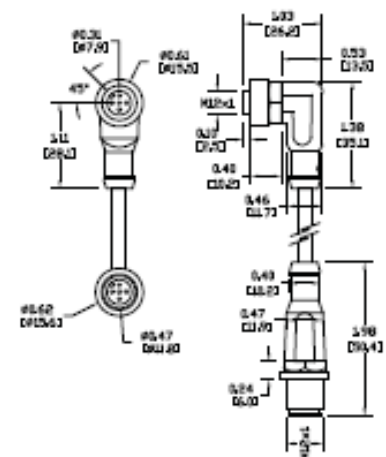


Figure 6



## **APPENDIX-F**

### **PIN DIAGRAM – PIC 18F4520**



**MICROCHIP**

**PIC18F2420/2520/4420/4520**

**28/40/44-Pin Enhanced Flash Microcontrollers with  
10-Bit A/D and nanoWatt Technology**

**Power Management Features:**

- Run: CPU on, Peripherals on
- Idle: CPU off, Peripherals on
- Sleep: CPU off, Peripherals off
- Ultra Low 50nA Input Leakage
- Run mode Currents Down to 11  $\mu$ A Typical
- Idle mode Currents Down to 2.5  $\mu$ A Typical
- Sleep mode Current Down to 100 nA Typical
- Timer1 Oscillator: 900 nA, 32 kHz, 2V
- Watchdog Timer: 1.4  $\mu$ A, 2V Typical
- Two-Speed Oscillator Start-up

**Flexible Oscillator Structure:**

- Four Crystal modes, up to 40 MHz
- 4x Phase Lock Loop (PLL) – Available for Crystal and Internal Oscillators
- Two External RC modes, up to 4 MHz
- Two External Clock modes, up to 40 MHz
- Internal Oscillator Block:
  - Fast wake from Sleep and Idle, 1  $\mu$ s typical
  - 8 use-selectable frequencies, from 31 kHz to 8 MHz
  - Provides a complete range of clock speeds from 31 kHz to 32 MHz when used with PLL
  - User-tunable to compensate for frequency drift
- Secondary Oscillator using Timer1 @ 32 kHz
- Fail-Safe Clock Monitor:
  - Allows for safe shutdown if peripheral clock stops

**Peripheral Highlights:**

- High-Current Sink/Source 25 mA/25 mA
- Three Programmable External Interrupts
- Four Input Change Interrupts
- Up to 2 Capture/Compare/PWM (CCP) modules, one with Auto-Shutdown (28-pin devices)
- Enhanced Capture/Compare/PWM (ECCP) module (40/44-pin devices only):
  - One, two or four PWM outputs
  - Selectable polarity
  - Programmable dead time
  - Auto-shutdown and auto-restart

**Peripheral Highlights (Continued):**

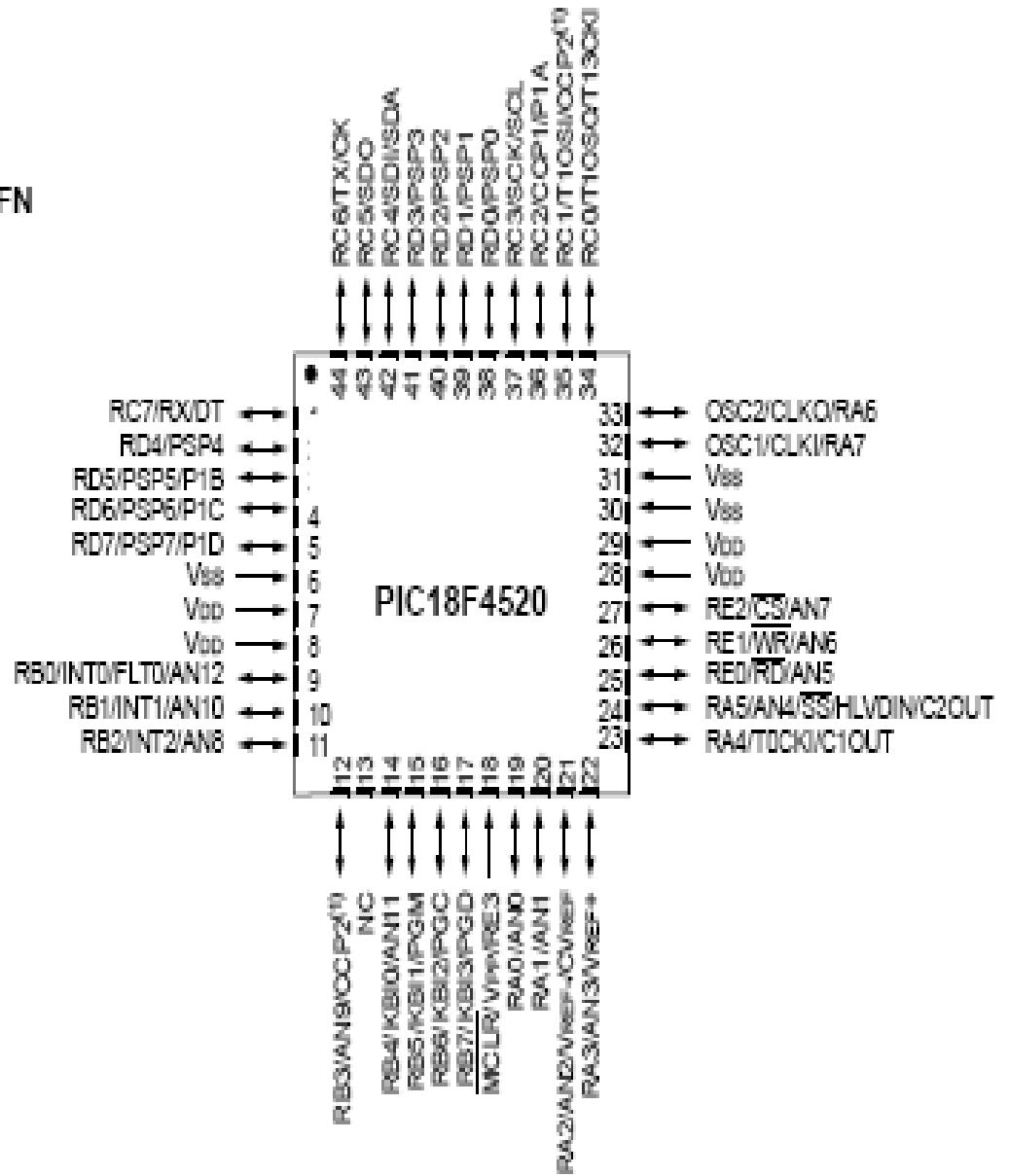
- Master Synchronous Serial Port (MSSP) module Supporting 3-Wire SPI (all 4 modes) and I<sup>2</sup>C™ Master and Slave modes
- Enhanced Addressable USART module:
  - Supports RS-485, RS-232 and LIN/J2602
  - RS-232 operation using internal oscillator block (no external crystal required)
  - Auto-wake-up on Start bit
  - Auto-Baud Detect
- 10-Bit, up to 13-Channel Analog-to-Digital (A/D) Converter module:
  - Auto-acquisition capability
  - Conversion available during Sleep
- Dual Analog Comparators with Input Multiplexing
- Programmable 16-Level High/Low-Voltage Detection (HLVD) module:
  - Supports Interrupt on High/Low-Voltage Detection

**Special Microcontroller Features:**

- C Compiler Optimized Architecture:
  - Optional extended instruction set designed to optimize re-entrant code
- 100,000 Erase/Write Cycle Enhanced Flash Program Memory Typical
- 1,000,000 Erase/Write Cycle Data EEPROM Memory Typical
- Flash/Data EEPROM Retention: 100 Years Typical
- Self-Programmable under Software Control
- Priority Levels for Interrupts
- 8 x 8 Single-Cycle Hardware Multiplier
- Extended Watchdog Timer (WDT):
  - Programmable period from 4 ms to 131s
- Single-Supply 5V In-Circuit Serial Programming™ (ICSP™) via Two Pins
- In-Circuit Debug (ICD) via Two Pins
- Wide Operating Voltage Range: 2.0V to 5.5V
- Programmable Brown-out Reset (BOR) with Software Enable Option

Device	Program Memory		Data Memory		IO	10-Bit A/D (ch)	CCP/ECCP (PWM)	MSSP		I <sup>2</sup> C (kbit/s)	Comp.	Timers @16-Bit
	Flash (bytes)	# Single-Word Instructions	SRAM (bytes)	EEPROM (bytes)				SPI	Master I <sup>2</sup> C™			
PIC18F2420	16K	8192	768	256	25	10	2/0	Y	Y	1	2	1/3
PIC18F2520	32K	16384	1536	256	25	10	2/0	Y	Y	1	2	1/3
PIC18F4420	16K	8192	768	256	35	13	1/1	Y	Y	1	2	1/3
PIC18F4520	32K	16384	1536	256	35	13	1/1	Y	Y	1	2	1/3

44-pin QFN



## **APPENDIX-G**

### **PIC C CODE FOR SILVERWARE SINGULATION**

```
//***** SILVERWARE SINGULATE CODE*****
```

```
//***** Include Files *****
```

```
#include<18f4520.h>
```

```
#include<string.h>
```

```
#include<stdlib.h>
```

```
#fuses HS,NOLVP,NOWDT,PUT
```

```
#use delay(clock=2000000)
```

```
#use rs232(baud=38400, parity=N, xmit=PIN_C6, rcv=PIN_C7,stream=HOSTPC)
```

```
//***** Define Output PINS *****
```

```
#define MOTOR_PIN PIN_C0
```

```
#define UPPER_MAGNET_PIN PIN_C1
```

```
#define LOWER_MAGNET_PIN PIN_C2
```

```
#define SHEET_SOLENOID_PIN PIN_C3
```

```
//***** Define Input Pins *****
```

```
#define UM_SENSOR PIN_A1
```

```
#define LM_SENSOR PIN_A2
```

```
#define SH_SENSOR PIN_A3
```

```
//***** Define Variables *****
```

```
#define ums input(UM_SENSOR)
```

```
#define lms input(LM_SENSOR)
```

```
#define shs input(SH_SENSOR)
```

```
#define ON 1
```

```
#define OFF 0
```

```

#define OBJ_PRESENT 1

#define OBJ_ABSENT 0

#define MOTOR_RUN 1

#define MOTOR_STOP 0

#define MAGNET_DISPENSE 0

#define MAGNET_BLOCK 1

#define SOLENOID_PULSE 1

#define SOLENOID_REST 0

#define SIGNAL_DELAY 150

#define MOTOR_DELAY 150

#define MOTOR_ON {output_toggle(MOTOR_PIN);}

#define MOTOR_OFF {output_low(MOTOR_PIN);}

#define UPPER_MAGNET_ON {output_high(UPPER_MAGNET_PIN);delay_us(MOTOR_DELAY);}

#define UPPER_MAGNET_OFF {output_low(UPPER_MAGNET_PIN);delay_us(SIGNAL_DELAY);}

#define LOWER_MAGNET_ON {output_high(LOWER_MAGNET_PIN);delay_us(SIGNAL_DELAY);}

#define LOWER_MAGNET_OFF {output_low(LOWER_MAGNET_PIN);delay_us(SIGNAL_DELAY);}

#define SHEET_SOLENOID_ON {output_high(SHEET_SOLENOID_PIN);delay_us(SIGNAL_DELAY);}

#define SHEET_SOLENOID_OFF {output_low(SHEET_SOLENOID_PIN);delay_us(SIGNAL_DELAY);}

//***** Define Size of Variables *****

int16 um_count=0,lm_count=0,sh_count=0,tt_count=0;

int time_scale1 = 0;

int um_s,lm_s,sh_s;

int mm_state,um_state,lm_state,sh_state;

int um_phy_state, lm_phy_state, sh_phy_state;

```

```

//***** Timer_0 Subcode *****

#INT_TIMER0

void timer0_isr()

{

set_timer0(61);

if (ums == OBJ_ABSENT) {MOTOR_ON; output_toggle(PIN_A5);} else {MOTOR_OFF;}

}

//***** Timer_1 Subcode *****

#INT_TIMER1

void timer1_isr()

{

set_timer1(3036); // timer overflows every 100ms ....

time_scale1 = time_scale1 + 1;

if (sh_count>(tt_count - sh_count)) sh_s = OBJ_PRESENT; else sh_s = OBJ_ABSENT;

if (um_count>(tt_count - um_count)) um_s = OBJ_PRESENT; else um_s = OBJ_ABSENT;

if (lm_count>(tt_count - lm_count)) lm_s = OBJ_PRESENT; else lm_s = OBJ_ABSENT;

lm_count = 0;

um_count = 0;

sh_count = 0;

tt_count = 0;

//**** Binary states of conveyor belt, electromagnets and solenoid and ****

if ((um_s == OBJ_ABSENT) && (lm_s == OBJ_ABSENT) && (sh_s == OBJ_ABSENT))

{mm_state=MOTOR_RUN; um_state = MAGNET_DISPENSE; lm_state = MAGNET_DISPENSE;}

```



```

else if ((um_s == OBJ_ABSENT) && (lm_s == OBJ_ABSENT) && (sh_s == OBJ_PRESENT))
{mm_state=MOTOR_RUN; um_state = MAGNET_DISPENSE; lm_state = MAGNET_BLOCK;}

else if ((um_s == OBJ_ABSENT) && (lm_s == OBJ_PRESENT) && (sh_s == OBJ_ABSENT))
{mm_state=MOTOR_RUN; um_state = MAGNET_BLOCK; lm_state = MAGNET_DISPENSE;}

else if ((um_s == OBJ_ABSENT) && (lm_s == OBJ_PRESENT) && (sh_s == OBJ_PRESENT))
{mm_state=MOTOR_RUN; um_state = MAGNET_BLOCK; lm_state = MAGNET_BLOCK;}

else if ((um_s == OBJ_PRESENT) && (lm_s == OBJ_ABSENT) && (sh_s == OBJ_ABSENT))
{mm_state=MOTOR_STOP; um_state = MAGNET_DISPENSE; lm_state = MAGNET_DISPENSE;}

else if ((um_s == OBJ_PRESENT) && (lm_s == OBJ_ABSENT) && (sh_s == OBJ_PRESENT))
{mm_state=MOTOR_STOP;um_state = MAGNET_DISPENSE; lm_state = MAGNET_BLOCK;}

else if ((um_s == OBJ_PRESENT) && (lm_s == OBJ_PRESENT) && (sh_s == OBJ_ABSENT))
{mm_state=MOTOR_STOP;um_state = MAGNET_BLOCK; lm_state = MAGNET_DISPENSE;}

else if ((um_s == OBJ_PRESENT) && (lm_s == OBJ_PRESENT) && (sh_s == OBJ_PRESENT))
{mm_state=MOTOR_STOP;um_state = MAGNET_BLOCK; lm_state = MAGNET_BLOCK;}

if (sh_s == OBJ_PRESENT) sh_state = SOLENOID_PULSE; else sh_state = SOLENOID_REST;

if (time_scale1 == 5) // 5 * 100ms ....
{
time_scale1 = 0;

// upper magnet pulsing ...

if (um_state == MAGNET_DISPENSE)
{
um_phy_state = 1 - um_phy_state;

if (um_phy_state == ON) {UPPER_MAGNET_ON;} else
{UPPER_MAGNET_OFF;}
}
}

```

```
else
{
    um_phy_state = ON;
    UPPER_MAGNET_ON;
}
// lower magnet pulsing ...
if (lm_state == MAGNET_DISPENSE)
{
    lm_phy_state = 1 - lm_phy_state;
    if (lm_phy_state == ON) {LOWER_MAGNET_ON;} else
    {LOWER_MAGNET_OFF;}
}
else
{
    lm_phy_state = ON;
    LOWER_MAGNET_ON;
}
}
// solenoid pulsing logic ....
if (sh_state == SOLENOID_PULSE)
{
    sh_phy_state = 1 - sh_phy_state;
    if (sh_phy_state == ON) {SHEET_SOLENOID_ON;} else
    {SHEET_SOLENOID_OFF;}
}
else
{
```

```

    sh_phy_state = OFF;

    SHEET_SOLENOID_OFF;

}

}

//***** Main Program *****/

void main(void)
{
    int done=0;

    set_tris_C(0x00);
    set_tris_A(0x0f);

    fprintf(HOSTPC, "\n\n\nr-----");
    fprintf(HOSTPC, "\n\nrProgram Started !! .... \n\nr");

    fprintf(HOSTPC, "\n\n\nr~~~~~");

//***** Declare Timer Variables *****/

    setup_timer_1(T1_INTERNAL|T1_DIV_BY_8);
    enable_interrupts(INT_TIMER1);

    setup_timer_0(RTCC_INTERNAL|RTCC_DIV_1);
    enable_interrupts(INT_TIMER0);
    enable_interrupts(GLOBAL);

    set_timer1(3036);

```

```
fprintf(HOSTPC, "\n\rSingulation Started ... Press ESC to quit.\n\n\r\n\r\n");
```

```
SHEET_SOLENOID_OFF;
```

```
UPPER_MAGNET_ON;
```

```
LOWER_MAGNET_ON;
```

```
sh_phy_state = OFF;
```

```
um_phy_state = ON;
```

```
lm_phy_state = ON;
```

```
output_low(PIN_B5) ;
```

```
output_low(MOTOR_PIN);
```

```
    while(done==0)
```

```
    {
```

```
        if (ums==1) um_count = um_count + 1; else um_count=0;
```

```
        if (lms==1) lm_count = lm_count + 1; else lm_count=0;
```

```
        if (shs==1) sh_count = sh_count + 1; else sh_count=0;
```

```
        tt_count = tt_count + 1;
```

```
    }
```

```
}
```

## **APPENDIX-H**

### **DATASHEET FOR MOTOR BELT DRIVE**

# WONDERMOTOR

YOUR SOURCE OF HIGH QUALITY MOTORS

[ E-mail: [sales@wondermotor.com](mailto:sales@wondermotor.com) ] [ Phone:  626.322.9220  ]



All of our products are sold through ebay. Please visit our ebay [store](#) to order our products. For products that are listed here but not on our ebay store site, simply [e-mail](#) us to request for your order(s). We also welcome wholesale/resale buyers.



## Electric Gear Motor 24v Low Speed 50 RPM Gearmotor DC

Rated Voltage: 27 VDC

Rated Speed: 50 RPM

Rated Load: 60 Watts

Rated Torque: 11.5 N-m (8.5 ft-lb)

Mounting: M6 screw holes

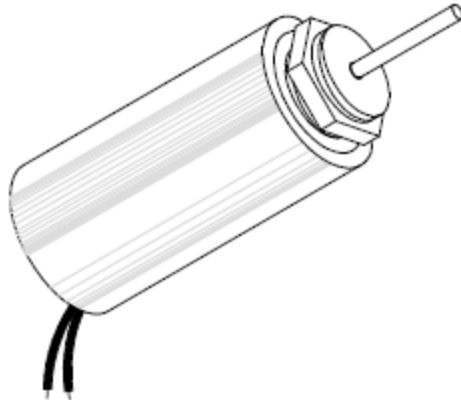
Shaft: 10mm shaft with 2 flats where flat to flat is 6.6mm and threaded end to fit a M6 tightening nut.

## **APPENDIX-I**

### **DATASHEET FOR THE SOLENOID**

# MAGNETIC SENSOR SYSTEMS

## *Push Type Tubular Solenoid*



**Series S-25-125-H**  
**1 1/4" DIA X 2 1/2"**

TOTAL WEIGHT: 11.2 OUNCES  
 PLUNGER WEIGHT: 1.5 OUNCES

duty cycle		1	1/2	1/4	1/10
maximum "ON" time, (Sec.)		∞	410	100	30
watts		11	22	44	110
approximate ampere turns		1410	2000	2820	4460
<b>AWG number</b>	<b>resistance</b>	<b>volts DC</b>	<b>volts DC</b>	<b>volts DC</b>	<b>volts DC</b>
20	0.97	3.2	4.5	6.3	10.0
21	1.38	4.0	5.6	7.9	12.5
22	2.49	5.1	7.2	10.2	16.1
23	3.49	6.2	8.8	12.5	19.7
24	6.06	8.1	11.5	16.2	25.5
25	9.89	10.3	14.5	20.5	32.4
26	16.6	13.0	18.4	25.9	41.0
27	24.5	16.1	22.8	32.2	50.9
28	36.9	20.4	28.9	40.8	64.5
29	61.8	25.5	36.1	51.0	80.6
30	93.3	31.5	44.6	62.9	99.5
31	144	40.3	57.1	80.6	127
32	210	49.4	70.0	98.7	156
33	357	63.5	90.0	127	201
34	553	82	116	164	259
35	993	105	149	210	332
36	1460	131	186	263	415
37	2406	160	227	320	506

HEAT SINK: For proper heat dissipation, body of solenoid should be mounted on an equivalent of 6.0" x 6.0" x 1/8" aluminum plate in an unrestricted flow of air.

---

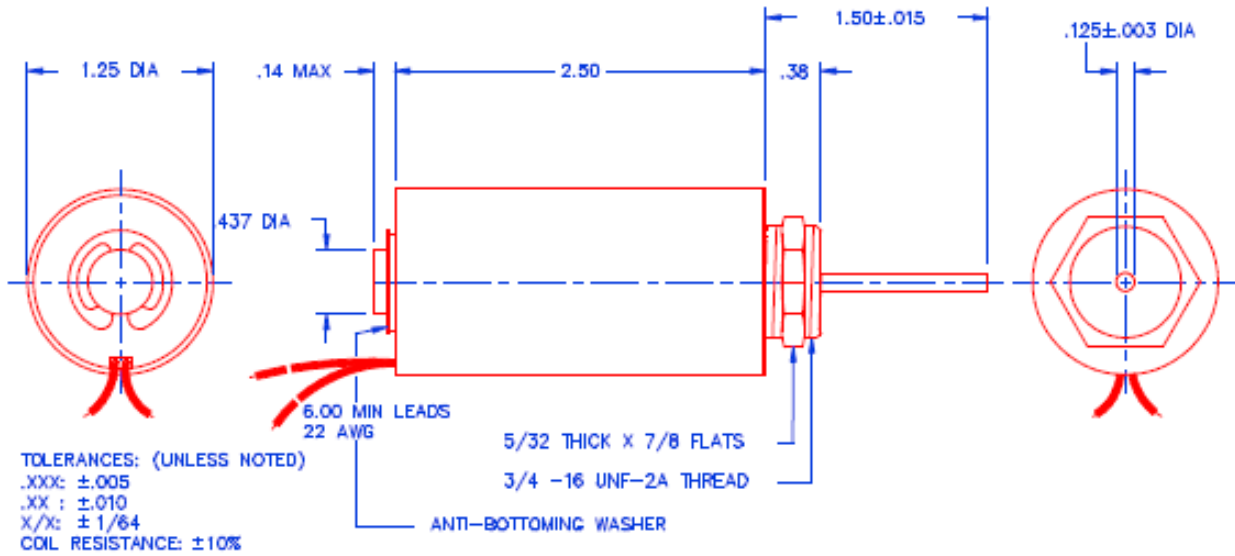
6901 Woodley Avenue, Van Nuys, California 91406  
 Telephone: (818) 785-6244 Fax: (818) 785-5713  
[www.solenoidcity.com](http://www.solenoidcity.com)



# MAGNETIC SENSOR SYSTEMS

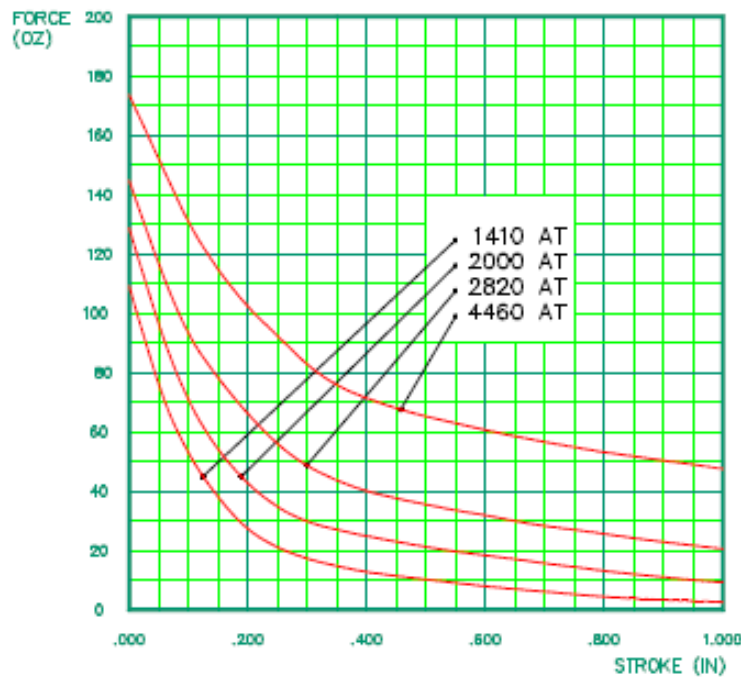
S-25-125-H

## MECHANICAL DIMENSIONS



SOLENOID SHOWN ENERGIZED

## TYPICAL PUSH FORCE VERSUS STROKE



## VITA

Rajashekar Reddy Chitaveli

Candidate for the Degree of

Master of Science

Thesis: SILVERWARE SINGULATION SYSTEM

Major Field: Mechanical and Aerospace Engineering

### Biographical:

Personal Data: Born in Thummala, Andhra Pradesh, India on 25th June 1985, son of Lakshmi Reddy Chitaveli and Chenna Krishnamma.

### Education:

Completed the requirements for the Master of Science in your Mechanical and Aerospace Engineering at Oklahoma State University, Stillwater, Oklahoma in December, 2011.

Received the Bachelor of Engineering in Mechanical Engineering at Visvesvaraya Technological University, Bangalore, India in 2007.

### Experience:

Software Engineer II, Sterling Commerce, from July, 2007 to December 2008.

Graduate Teaching Assistant, Department of Mechanical and Aerospace Engineering, OSU from January, 2009 to December, 2010.

Graduate Research Assistant, College of Education, OSU from December, 2010 to December, 2011.

### Professional Memberships:

Member, International Society of Automation, 2011